ADVANCED FUNCTIONAL MATERIALS
www.afm-journal.de

Recent Progress of Conductive Hydrogel Fibers for Flexible Electronics: Fabrications, Applications, and Perspectives

Wanwan Li, Jiao Liu, Jingnan Wei, Zhaoyan Yang, Chunlei Ren, and Bingxiang Li**

Flexible conductive materials with intrinsic structural characteristics are currently in the spotlight of both fundamental science and advanced technological applications due to their functional preponderances such as the remarkable conductivity, excellent mechanical properties, and tunable physical and chemical properties, and so on. Typically, conductive hydrogel fibers (CHFs) are promising candidates owing to their unique characteristics including light weight, high length-to-diameter ratio, high deformability, and so on. Herein, a comprehensive overview of the cutting-edge advances the CHFs involving the architectural features, function characteristics, fabrication strategies, applications, and perspectives in flexible electronics are provided. The fundamental design principles and fabrication strategies are systematically introduced including the discontinuous fabrication (the capillary polymerization and the draw spinning) and the continuous fabrication (the wet spinning, the microfluidic spinning, 3D printing, and the electrospinning). In addition, their potential applications are crucially emphasized such as flexible energy harvesting devices, flexible energy storage devices, flexible smart sensors, and flexible biomedical electronics. This review concludes with a perspective on the challenges and opportunities of such attractive CHFs, allowing for better understanding of the fundamentals and the development of advanced conductive hydrogel materials.

1. Introduction

During the last few decades, the flexible electronics are undergoing the staggering speed of advancements, which are omnipresent in the contemporary life ranging from flexible displays, touch panels, electronic skin, soft robotics, wearable energy devices, human-machine interactions, flexible sensors to real-time health-monitoring devices.[1–8] Compared to the traditional rigid and brittle silicon-based electronics, flexible electronics manifesting the peculiar characteristics, such as miniaturized, lightweight, portable, foldable, stretchable, and biocompatible are triggering the intense interests of researchers from multidisciplinary fields like biology, material science, and chemistry.[9–11] Nowadays, great attempts have been devoted to developing advanced flexible electronics by integrating various inorganic or organic traditional conductive functional materials with flexible electrochemically non-active elastic substrates.[12–17] Generally, traditional conductive functional materials encounter the shortcomings such as high price, inherent rigidity, weak biocompatibility, poor mechanical, and inferior interface bonding properties, which are employed to evaluate the performance of the flexible electronics materials. Therefore, pursuing these materials with practical applications is an emergent issue in the research field.

Nevertheless, in numerous conductive functional materials, hydrogels with 3D network structures have been largely selected as the excellent candidates due to their high water content, excellent biocompatibility and biodegradability properties, high elasticity, and outstanding stimulus responsiveness.[18–23] Conductive hydrogels are generally constructed via integrating various conductive substances into the hydrogel matrix, which are comprised of carbon materials (carbon nanotubes (CNTs), graphite), metal oxides, metal sulfides, metal nanoparticles and conductive polymers (polyaniline (PANI), polypyrrole (PPy), poly (3,4-ethylenedioxythiophene) (PEDOT:PSS)).[24–30] For example, Han et al. fabricated a CNTs-based conductive hydrogel for strain sensors by in situ polymerization of acrylic acid and acrylamide in water/glycerol solutions in the presence of polydopamine-decorated CNTs.[28] Devaki et al. reported a 3D Ag nanoparticles-polyacrylic acid conductive hydrogel via combining in situ polymerization of acrylic acid and reduction of Ag^+.[29] Duan et al. constructed a robust and force-sensitive conductive hydrogel employing synthesizing polyacrylamide and PANI in closely packed swollen chitosan microspheres.[30] According to the different configurations of hydrogels, conductive hydrogels are allowed to be processed into 3D bulk gels, 2D gel films, 1D gel fibers, and 0D microgels.[31–36] The mechanical flexibility of 1D fibrous configuration is superior to that of 3D bulk or 2D film configuration due to its well-oriented polymer chains, light weight, and low dimensions for flexible electronics. Moreover, ultra-flexible fibrous materials can be easily woven into diverse soft and breathable fabrics, which

W. Li, J. Wei, C. Ren
College of Textile
Zhongyuan University of Technology
Zhengzhou 450007, China
E-mail: ren@zut.edu.cn
J. Liu, Z. Yang, B. Li
College of Electronic and Optical Engineering & College of Flexible Electronics (Future Technology)
Nanjing University of Posts and Telecommunications
Nanjing 210023, China
E-mail: bxli@njupt.edu.cn
The ORCID identification number(s) for the author(s) of this article can be found under https://doi.org/10.1002/adfm.202213485.

DOI: 10.1002/adfm.202213485

can efficiently accommodate complex deformations, match the bending stiffness of biological tissues, and create a more comfortable wearable environment for the human skin. Thus, 1D conductive hydrogel fibers (CHFs) have become critical candidates as flexible function materials of flexible electronics on account of their unique features including anisotropy, large length-to-diameter ratio, good weavability and knittability, and excellent mechanical flexibility (**Figure 1**).[37–43]

The 1D macrostructures and 3D network microstructures of CHFs not only afford continuous and effective transport channels for electrons and ions, but also contract the diffusion distance of ions as well as accelerate the electrons and ions transport rate. It is noted that CHFs are preferable for flexible electronics in consequence of their high conductivity and electrochemical activity, involving the flexible energy harvesting and storage devices.[44–46] Intriguingly, 1D CHFs response quickly to small stimuli changes in the external environment such as temperature, strain, pressure, and humidity, which is important for the flexible smart sensors.[47] In addition, as extracellular matrix analogues, CHFs with tissue similarity and biocompatibility, can substantially enhance the cell adherence, culture and differentiation. Meanwhile, CHFs can act as a powerful interface linking the soft tissues of human bodies and electronic devices, allowing for the collection of various physiological signals for personal health management. Indeed, they are permitted to be employed in tissue engineering, soft robotics, implantable bioelectronics, and other fields.[48–57] Furthermore, CHFs possessing excellent mechanical flexibility and deformation resistance can better adapt the complex and changeable stress from the external environment on the basis of their unique porous structure and high porosity, thus satisfying the requirements of the stability of flexible electronics. Simultaneously, CHFs are able to be tailored facilely by weaving and integrating with different components into the fabric for the fabrication of wearable electronics. More importantly, the conductive network and microstructure of CHFs can be rationally designed at the molecular level to construct multi-functional materials and devices, such as anti-freezing, self-healing, shape memory, multiple stimulus responsiveness, etc., greatly extending the scope of their application range.

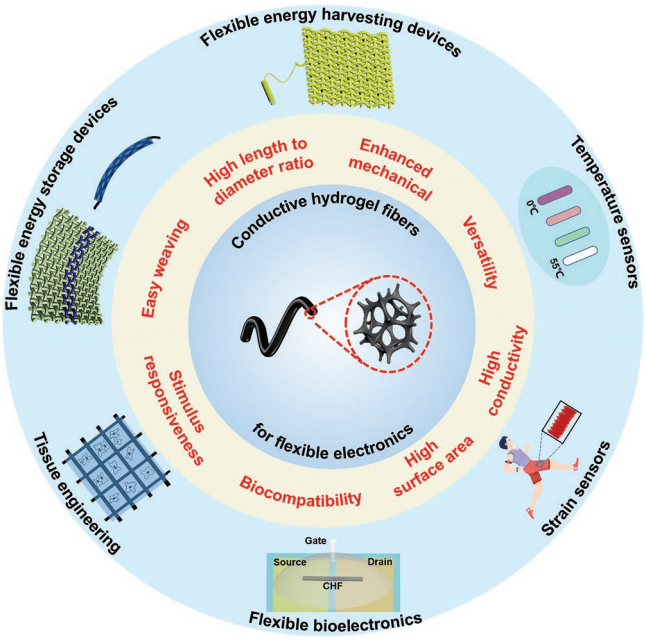

Figure 1. Schematic illustration of flexible electronics applications of CHFs. The red circle represents the enlargement illustration of the 3D network interior microstructure of CHFs for electrons and ions transportation, looking like 3D porous foam morphology.

So far, many reviews are probing into the design, fabrications, and applications of conductive hydrogels generally with 2D film or 3D bulk configurations in flexible electronics.[58–66] Parallelly, some reviews elucidate the applications of hydrogel fibers in biomedical engineering, such as tissue regeneration, wound healing, and drug delivery system.[67–72] It is of paramount significance to summarize the recent progress of CHFs-based flexible electronics, which probably facilitates the researchers to adequately understand this field. In this review, we give a systematic elaboration on the architectural features, function characteristics, construction strategies, and applications of CHFs in flexible electronics. To begin with, the architectural features, function characteristics, construction strategies, and underlying formation mechanisms of CHFs are introduced. Then an overview of the applications of CHFs in flexible electronics are showcased, which include flexible energy harvesting and storage devices, flexible smart sensors, and flexible biomedical electronics. Finally, we conclude this review with a perspective on the challenges, opportunities, and the future research directions of CHFs-based flexible electronics. It is anticipated that this review can not only provide the deep the understanding of the fundamentals of sorts of conductive hydrogel materials, but also bring new insight in the development of designing more innovative conductive hydrogel materials and exploiting more fabrication techniques for CHFs for their promising applications in the fields of flexible electronics.

2. The Architectural Features and Function Characteristics Of CHFs

In this section, we will discuss the substantial merits of CHFs, such as large length-to-diameter ratio, easy weaving, excellent mechanical properties, high specific surface area, high water content, high conductivity, stimulus responsive, biocompatibility, self-healing, anti-freezing, and water retention on account of their architectural features and function characteristics (**Figure 2**).

2.1. The Architectural Features

2.1.1. 3D Network Structures

Mimicking the structural and functional characteristics of extracellular matrix of natural tissue, the uniquely 3D network structures of CHFs formed by hydrophilic polymer chains impart CHFs with high specific surface area and high water content, which can create a suitable microenvironment for cell proliferation, differentiation, and maintenance. The high water content of CHFs facilitates the exchange of biological molecules and

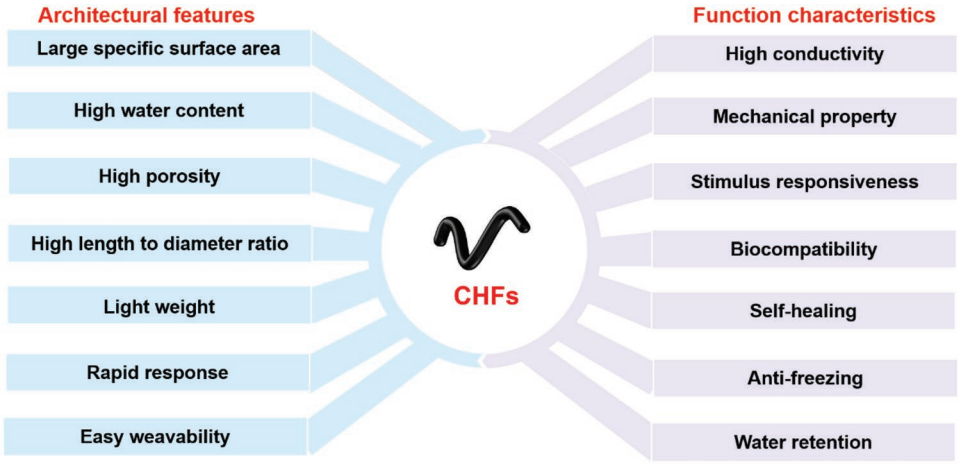

Figure 2. A guiding figure for the architectural features and function characteristics of CHFs.

markers across interfaces in biomedical field.[32,73] In addition, the 3D network structures of CHFs with a high degree of compactness facilitate to achieve rapid response, namely, subtle structural changes of the microstructure domain can be quickly transmitted to the adjacent domains, which can be applied as sensors.[74,75] Moreover, CHFs have been widely adopted as fiber electrodes in flexible energy devices owing to their uniquely 3D porous network structures and high conductivity.[38,62] In the first place, the stable 3D porous network structures acting as conductive frameworks not only provide continuous fast transport channels for electrons and ions, but also possess a large effective surface area to contact and diffuse ions, thus improving the utilization of the electrode materials. In another, CHFs can offer favorable interfaces between electrodes and electrolytes and facilitate fast and efficient electrochemical reactions as a result of their 3D network structural superiority of accommodating a large amount of ionic liquid. What's more, 3D porous structures of CHFs contribute to drastically resist the volume expansion or shrinkage and greatly maintain mechanical integrity of electrode materials during charging and discharging process, which is vital performance indicators for energy devices. For instance, Teng et al. constructed a hierarchically 3D interconnected porous PEDOT:PSS/PPy hybrid CHF via hydrothermal assembly of PEDOT:PSS solution and in situ chemical oxidative polymerization of pyrrole.[76] Benefiting from its hierarchically 3D porous nanostructure, high conductivity, strong π–π interaction and good flexibility, this CHF demonstrated fast electrons transfer/ions diffusion and the efficient utilization of whole electrode, which could be assembled into the fiber supercapacitor with the superb specific capacitance and the excellent rate performance. In addition, CHFs can effectively adapt to complex deformations from outside environment via changing their 3D network structures and behaviors during their own execution. More importantly, a variety of properties of CHFs, including conductivity, mechanical properties, self-healing, anti-freezing, and other multifunctionality, could be precisely regulated to satisfy actual application demands via the rational design of network structures, compositions, and molecular interactions of hydrogels. Hence, the 3D network structures of CHFs are crucial to their performance of all sides.

2.1.2. 1D Fiber Structures

Compared to 2D hydrogel films or 3D hydrogel monoliths, 1D CHFs with considerable dominances of small cross-sectional areas, high length-to-diameter ratio, well-oriented polymer chains, light weight, and faster mass transfer, not only more quickly respond to external stimulus, but also bear more tensile force under the same load.[67,77]Apart from that, CHFs exhibit enhanced mechanical properties and specific anisotropies thanks to their oriented condensed structures that the polymer chains align along the longitudinal direction. As for wearable devices, conventional 3D or 2D electronics fail to efficiently meet the requirements of flexibility and breathability mainly due to their intrinsic rigidity and bulkiness. To overcome this challenge, various CHFs-based flexible electronics have been developed considering their superiority of small diameter, lightweight, wonderful flexibility, easy weavability, and fantastic reconstruction ability into various hierarchical architectures. On one hand, they can efficiently accommodate complex deformations via a series of changes including twisting, bending, and stretching. On the other hand, CHFs with diameters ranging from tens to hundreds of micrometers can be arbitrarily woven into various 3D or 2D textiles and fabrics using textile techniques such as knitting, weaving, and embroidery or can be integrated into daily clothing to build perfectly conformal contacts with human skin, which can be served as wearable sensors to detect human motions and physiological signals rapidly and sensitively. For example, Li et al. reported ionic polyimide CHFs based on strong ion complexation interactions between calcium ions and carboxylate groups via wet spinning.[78] They demonstrated an excellent conductivity of ≈21 mS cm^{-1} and outstanding mechanical properties with a tensile strength of 2.5 MPa and breaking elongation of 215% owing to their ion-rich property and robust skeletal structure. They were easily woven and assembled to form integral wearable textiles for applications in wearable and flexible strain sensors with high sensitivity and good cycling stability under diverse complex environments. With regard to their applications in implantable biomedical devices, CHFs with miniaturized and flexible features can not only act as a better carrier

environment to encapsulate cells and load different therapeutic drugs or molecules for tissue engineering, but also are applicable to be deeply penetrated and easily retrieved into tissues during the minimally invasive surgical procedures free from biomedical complications.[79,80] Overall, CHFs can effectively overcome the mechanical mismatch between the hydrogels and human tissues and avoid the large size and isotropic structure of the hydrogels to hinder their responsiveness and sensitivity based on the combination of the 3D network microstructure and 1D macrostructure.

2.2. The Functional Characteristics of CHFs

2.2.1. High Conductivity

Conductivity is the most critical characteristic of CHFs. The conductivity of CHFs is aroused by the movement of electrons or ions in the 3D network structures of hydrogels. Generally, conductive hydrogels are fabricated in two strategies: 1) Conductive hydrogel network with the single component is constructed via self-polymerization or self-assembly of conductive polymers/fillers; 2) Conductive hydrogel network is integrated into existing non-conductive hydrogel matrix via introducing interpenetrating conductive networks or various conductive substances, such as conductive polymers, conductive fillers, and free ions.[81,82] In the light of conductive mechanisms, CHFs can be categorized into electronic, ionic, and hybrid electronic-ionic CHFs. Conductive polymer-based CHFs, including PEDOT, PANI, and PPy, belong to electronic CHFs on the grounds of their electronic conduction induced by the conjugated π bond of the conductive polymers. Conductive fillers-based CHFs primarily depend on electronic conduction of the conductive fillers, such as graphene, CNTs, and metal nanoparticles. For example, Yao et al. prepared a PEDOT:PSS CHF in a glass capillary by thermal treatment of a commercial PEDOT:PSS suspension in 0.1 mol L^{-1} sulfuric acid followed by partially removing its PSS component with concentrated sulfuric acid.[83] This dried CHF demonstrated an extremely high conductivity of 38 000 S m^{-1}, a strong tensile strength of 280 MPa, and a large failure strain of 14.6%, which could be used as the fiber electrode to fabricate a current-collector-free fiber supercapacitor. However, the inherently rigid conductive fillers inevitably cause the trade-off between the mechanical compliance and the conductivity of CHFs, since the high amounts of conductive fillers approaching the percolation threshold often lead to the increase of fiber's Young's modulus and the decrease of their stretchability. Moreover, these rigid conductive fillers have a mismatched modulus with the hydrogel matrixes, easily leading to the interfacial delamination in the fibers during repeated stretching. Furthermore, electronic CHFs are usually opaque, black, and have a small fracture strain, which will limit their usage in the practical applications.

Inspired by ion transportation nature of living systems, the burgeoning ionogel fibers composed of a 3D polymer network percolating through the ionic liquid (IL), mediating signal by mobile ions, have gained tremendous interest recently. Distinct from tradition conductive fillers, IL can realize good dispersion in the polymer matrix owing to the noncovalent interactions between IL and polymers in ionogel fibers. Consequently, ionogel fibers can support high loading of IL, giving rise to high ionic conductivity without sacrificing their stretchability. Ionogel fibers possess considerable unique advantages, such as good optical transparency, tissue-matchable moduli, tunable mechanical properties, high molecular designability, high stability over a wide temperature range, and non-flammability, which have offered great opportunities for the development of bioelectronics, soft robotics, sensors, energy harvesting, electronic skin, and ionic cables.[84–87] For example, Sun et al. reported a highly stretchable, transparent, and self-healing ionogel fiber based on double physical crosslinking including hydrogen bonding and dipole–dipole interaction using tubular Teflon mold.[87] This ionogel fiber easily woven with ordinary fabrics could be used as a strain sensor for human motion monitoring because of its mechanical adaptability, and a thermal sensor due to the temperature dependence of conductivity, which demonstrated great potential in wearable electronics. CHFs represent tailorable conductivity according to different application requirements via designing electronic, ionic, or hybrid conductive network. Typically, CHFs with high conductivity are rarely used in the biomedical field, but widely used in the sensors or energy devices. The reason is that CHFs with low ionic conductivity are sufficient to transmit bioelectrical signals and electrically stimulate cell proliferation and differentiation in vivo matching with the rather low microcurrent intensity in the human body. The high concentrations of salt ions may reduce the biocompatibility of hydrogels, thus limiting their applications in bioelectronics. Contrarily, the high conductivity confers CHFs as electrodes with improved electrochemical performance because of the fantastic ions/electrons transmission capability.

Enhanced conductivity of CHFs has great implications for extending their application ranges. There are three directions to enhance the conductivity of CHFs from the perspectives of conductive mechanisms of CHFs. First, the conductivity can be improved by introducing conductive polymers to form a conjugated skeleton through in situ polymerization on the basis of the original network. Moreover, increasing the amounts of conductive polymer contributes to increase the electron concentration in the hydrogel system, leading to the improvement of the conductivity of CHFs. However, the mechanical properties of CHFs may be damaged by reason of the inherently rigid conjugated structure of conductive polymers. Second, the conductivity of CHFs can also be enhanced by integrating conductive fillers into the hydrogel network based on various molecular interactions, including π–π stacking interactions, hydrophobic effect, and hydrogen bonding because of the increased charge transport channels. Nonetheless, too many fillers may give rise to the phase separation between hydrogel matrix and fillers, thus deteriorating the stretchability of CHFs. Third, the additional of salt ions into the pores of the hydrogel network can elevate the conductivity of ionic CHFs via infiltration benefiting from the enhancement of the charge transfer efficiency.

2.2.2. Mechanical Properties

Mechanical properties are also significant characteristics of CHFs, including elasticity, toughness, and stretchability. It is

inevitable that wearable devices are often subjected to various external forces induced by the complexity of the motion of human and external environment in practical applications, including stretching, bending, twisting, compression, and folding. As a consequence, excellent mechanical properties of CHFs are considered as crucial parts for designing the devices, which are required to maintain the high performance of devices. Similar to the conductivity of CHFs, the mechanical properties of CHFs can be designed to satisfy a variety of requirements in different applications. In general, high mechanical properties of CHFs are required in energy devices and sensors applications, such as tensile, compressive and flexible. For the biology applications, the Young's modulus of CHFs is consistent with that of biological tissues so that they can effectively achieve electrical stimulation and sustain their integrity of 3D structure and function. Moreover, CHFs can be regulated to form diverse mechanically compliant interfaces with a variety of biological tissues, minimizing their mechanical mismatch with biological tissues.[23]

Recently, various tactics have been excavated to improve the mechanical properties of CHFs. Double network crosslinking, which is regarded as a representative method, is widely employed to fabricate CHFs with high toughness and excellent stretchability. The double network structure is made up of two contrasting and interpenetrating polymer networks with opposite mechanical properties. The first network with densely crosslinked creates CHFs stiff and brittle while the second network with sparsely cross-linked makes CHFs soft and stretchable. Once CHFs are subjected to stress, the internal fracture of brittle first network happens dissipating large amounts of energy during large deformations, while the flexible second network can supply elasticity to maintain their structure integrity. The unique energy dissipation mechanism of double network structure expectedly reinforce mechanical properties of CHFs. Inspired by muscle architectures, Geng et al. reported double network hydrogels with hierarchically aligned structures composed of cross-linked cellulose nanofiber/chitosan hydrogel fibers and poly (acrylamide-co-acrylic acid).[88] After further cross-linking using Fe^{3+}, the hydrogel demonstrated an outstanding mechanical performance with an average strength of 11 MPa and elongation-at-break of 480% owing to the effective energy dissipation of the oriented asymmetric double network, which showed promising potential in biological applications. Another way to enhance the toughness and stretchability of CHFs is to design and construct proper covalent or noncovalent interactions among the hydrogel networks, polymer chains and the conductive fillers, which are related to their mechanical properties. Meanwhile, appropriately increasing the amount of salt ions and conductive fillers in hydrogels contributes to boost the mechanical properties of CHFs. In practical applications, the mechanical properties and conductivity of CHFs need to be balanced. **Table 1** lists the representative examples of CHFs in terms of materials, conductivity and mechanical performance.

Table 1. Representative examples of CHFs with regard to the conductivity and the mechanical performance.

Types of CHFs	Materials	Conductivity	Mechanical performance (tensile strength, strain)	Reference
Electronically	PEDOT:PSS	38 000 S m^{-1}	280 MPa, 14.6%,	[83]
CHFs	PANI/PA/GO	–	140 MPa, 31%,	[89]
	PEDOT/PANI	200 S cm^{-1}	120 MPa, 7%,	[90]
	RGO-PEDOT: PSS-PVA	114 S m^{-1}	–	[91]
	$Ti_3C_2T_x$ MXene aerogel	104 S m^{-1}	1.1 MPa, 0.35%	[92]
	PEDOT:PSS@PVA	0.00163 S cm^{-1}	13.76 MPa, 519.9%.	[93]
Ionically CHFs	Polyimide	21 mS cm^{-1}	2.5 MPa, 215%	[78]
	PAAS-PMA	2 S m^{-1}	5.6 MPa, 1200%	[94]
	PAAm/PAMPS	–	5.6 MPa, 159%	[95]
	P(NAGA-co-AAm)	0.69 S m^{-1}	2.27 MPa, 900%	[55]
	P(AAm-co-PAA)/ Fe(III)	4.2 mS m^{-1}	0.27 MPa, 500%	[96]

2.2.3. Stimulus Responsiveness

Stimulus responsive hydrogels, referred to as intelligent hydrogels, can sense and respond to changes in the external environment, which have broad potential applications in the field of micro-environmental sensing.[97] Similar to stimulus responsiveness of organisms, CHFs can integrate sensing, driving, and information processing to display intelligent properties. The external stimulations generally are external physical and chemical factors, including temperature, pH, light, electricity, magnetism, sound, force, and chemicals.[98–100] The stimulus responsiveness mechanism of CHFs is that the microstructural and the interaction force between internal chains and chains or conductive fillers of hydrogels change at the molecular level when they suffer from various external stimulations, ultimately resulting in the variation of the overall characteristics of CHFs. For example, the network based on weak electrostatic interactions will be affected by temperature. The microscopic forces of the hydrogel network vary from the changes of temperature, thus affecting the overall performance of hydrogels. Additionally, responsive conductive hydrogels playing the role of conveying different electrical signals because they show different electrical conductivities to different external environments. Thus, CHFs can serve as an ideal bridge to transmit electrical signals between the human body and electronics. More importantly, 1D CHFs demonstrate higher sensitivity because of their small diameters and large length-to-diameter ratio, which exhibit promising application prospects in the future. Li et al. fabricated $Ti_3C_2T_x$ MXene aerogel fibers with an intriguing oriented mesoporous structure via a simple dynamic sol-gel spinning and subsequent supercritical CO_2 drying.[92] These $Ti_3C_2T_x$ MXene aerogel fibers exhibited the ultrahigh conductivity up to 10^4 S m^{-1} and the high specific surface area up to 142 m^2 g^{-1}. They displayed excellent electrothermal/photothermal dual-responsiveness due to the high electrical conductivity and the remarkable light absorption ability, which showed potential in flexible wearable devices, smart fabrics, and portable equipment applications. To conclude, responsiveness further confers

CHFs-based flexible devices with controllability, changeability, and multiplicity, which remarkably expands the application ranges of CHFs, such as flexible sensing, soft robots, energy storage, microfluidics and biomedical fields.

2.2.4. Other Functions

In addition to the above properties containing conductivity, mechanical, and stimulus responsiveness, other prominent properties of biocompatibility, self-sealing, an-freezing, and water retention have also become indispensable parts of CHFs for flexible electronics.[59,63,101–103] Ordinarily, biocompatibility is the most basic features for flexible electronics in human health-related applications, especially those integrated on the clothing or implanted devices. Mimicking the intrinsic morphologies and functions of human tissues, multifunctional CHFs possess unique biological properties, such as biocompatibility, biodegradability, tissue adaptability (well-matching biological tissues in terms of bending stiffness), and minimal invasiveness.[104] The biocompatibility of CHFs can keep the human body from a series of immunogenic responses and non-toxic side effects, which can trigger inflammation, insecurity, and allergic reactions in the body. Flexible electronics are often inevitably subjected to damage under long-term use and external stress from the environment, self-healing can make CHFs recover their structure integrity and performance after damage, and prolong the service life and durability of the devices. The self-healing mechanism of CHFs is based on various reversible molecular interactions consisting of dynamic covalent bonds and dynamic non-covalent bonds, such as hydrogen bonding, electrostatic ionic forces, host-guest interactions, and hydrophobic bonding.[101,105] CHFs based on dynamic covalent bonds can achieve self-healing via breaking and re-forming covalent bonds by means of proper external conditions (eg. temperature, pH or light). It is expected that CHFs based on dynamic non-covalent bonds can reconstruct hydrogel structure without any external conditions. In short, self-healing of CHFs deriving from these existences of dynamic bonds can notably boost the stability of CHFs-based flexible electronics.

Anti-freezing is another important property of CHFs, especially in extreme low temperature environments. CHFs with abundant water can freeze below zero degrees, causing the shape change of hydrogels, making the network structures fragile, and destroying the ions transport channels, thus leading to the exacerbations of flexibility and conductivity of CHFs. Developing anti-freezing CHFs can effectively overcome the above difficulties and significantly expand their applications at low temperatures.[106,107] To lower the freezing point of CHFs is an effective mean to prevent freezing. There are two ways to fabricate anti-freezing CHFs. The common strategy is to introduce various cryoprotectants to CHFs via a simple solvent replacement, such as ethylene glycol, glycerol, and sorbitol, inhibiting the nucleation and regeneration of ice crystals of supercooled water. Another way is to add inorganic salts to CHFs to lower the liquid–solid transition temperature and prevent the hydrogel freezing phenomenon to a certain extent, such as Na^+, Cl^-, Li^+, Ca_2^+, and other salt ions. Apart from that, water inside CHFs is susceptible to evaporate in the dry environment, resulting in the dysfunction of devices. In order to overcome this challenge, constructing organohydrogels fiber system by solvent displacement method or using binary solvent as dispersion medium can reduce the vapor pressure of CHFs, thus preventing them from drying out. Additionally, coating as-fabricated CHFs with a thin hydrophobic layer, for example, polymethyl acrylate (PMA), polydimethylsiloxane (PDMS) and Ecoflex, can physically reduce the rate of water evaporation, which is also an effective approach to preserve water in CHFs.[63,103,108] Shi et al. constructed the nonvolatile, stretchable, and adhesive ionogel fibers using the ionic liquid 1-ethyl-3-methylimidazolium dicyanamide ([EMIM][DCA]) as the only dispersion medium, and Zwitterionic [2-(Methacryloyloxy) ethyl] dimethyl-(3-sulfopropyl) (SBMA) and acrylamide (AM) as monomers via mold method based on the ion-dipole, dipole–dipole interactions and interchain hydrogen bonds.[93] The P(SBMA-co-AM) ionogel fibers successfully overcame the problems of dehydration at high temperature and icing at subzero temperature due to the inherent non-volatility, low freezing point of ionic liquid and enhanced anti-freezing performance caused by ion-dipole interaction. This ionogel-fiber based sensor worked well in harsh environments, exhibiting an enlarged working temperature range from −80 to 150 °C and high tolerance under vacuum of 1.325 kPa. Overall, CHFs represent excellent conductivity, tunable mechanical performance, significant stimulus responsiveness, considerable biocompatibility, self-healing, anti-freezing, and water retention, which lay the foundations for their application as all kinds of flexible electronics.

3. Fabrication of CHFs

Hydrogel fibers with ordered chain alignment demonstrate enhanced mechanical and electrical properties than 2D hydrogel films and 3D hydrogel monoliths with random orientation and disordered alignment of the polymer chains, which show huge potential and bright prospect in tissue engineering, biomedicine devices, and flexible electronics.[109–116] In the initial stage of development, most hydrogel fibers are constructed from less varieties of used spinnable polymers with high molecular weight and low viscosity, such as alginate, polyvinyl alcohol (PVA), polyoxyethylene (PEO) via traditional wet spinning, electrospinning, and 3D printing. The fiber fabrication techniques and applicable materials are commonly limited in consequence of poor spinnability of hydrogels or precursor solutions including monomers and oligomers with reaction activity, low molecular weight, and viscoelasticity, resulting in poor mechanical properties or requiring complex extra crosslinking processes. Besides, the obtained hydrogel with the crosslinking structure is difficult to withstand the tensile deformation during fiber processing. In the view of hydrogel gelation process, it is a time-consuming and slow three-step approach including initiation, chain propagation, and totally crosslinking to form the crosslinking structure, which is largely inconsistent with the rapid spinning process of fiber formation. Consequently, realizing a coordinated effort of fiber forming and hydrogel gelation process, or the generation of fiber shapes and the cross-linking network simultaneously, is essential for successfully fabricating hydrogel fibers.

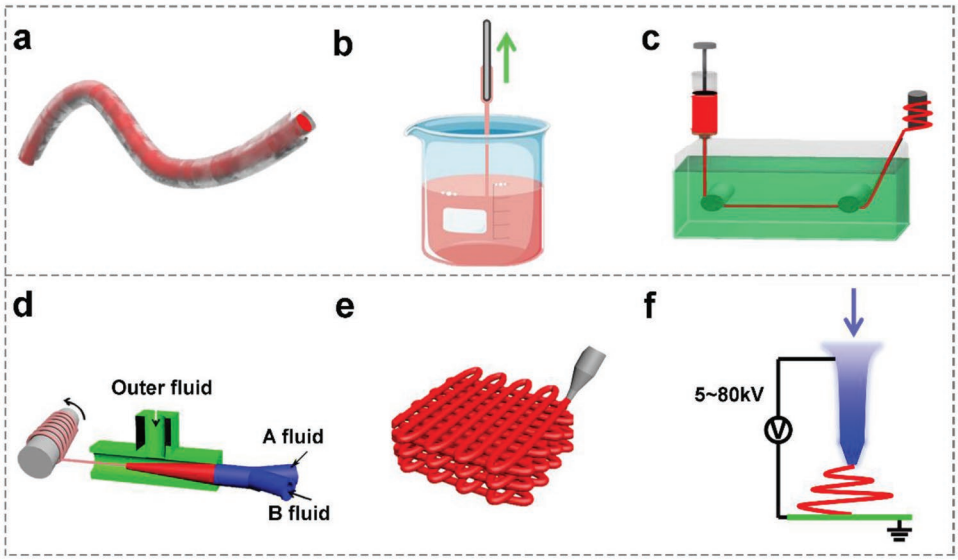

Figure 3. Schematic diagram of fabrication of CHFs. a) Capillary polymerization method. b) Draw spinning. c) Wet spinning. d) Microfluidic spinning. e) 3D printing. f) Electrospinning.

Over the past several decades, with tremendous endeavors of researchers, great progress in various fabrication approaches of hydrogel fibers have been achieved and numerous novel systematic strategies have been developed. According to the formation mechanism and the length of hydrogel fibers, the preparation methods of hydrogel fibers are categorized into discontinuous and continuous fabrication methods. The hydrogel fibers with finite length and controllable size were prepared conveniently by the discontinuous fabrication methods, including capillary polymerization, draw spinning, and extrusion spinning, without combining the gelation process with the fiber forming process. By contrast, continuous fabrication methods, including wet spinning, microfluidic spinning, 3D printing, electrospinning, dynamic polymerization spinning, and these techniques combined with various cross-linked strategies of hydrogels network, can remarkably synchronize the gelation process and the fiber formation process, finally construct continuously hydrogel fibers with random lengths. As a sort of hydrogel fibers, these designed strategies and preparation technologies can provide a useful reference for preparing CHFs (**Figure 3**). The detailed formation mechanisms of CHFs as well as merits and shortcomings of these fabrication are discussed below.

3.1. Discontinuous Fabrication Techniques

3.1.1. Capillary Polymerization Method

CHFs with limited length and controllable diameter can be fabricated in a specific capillary mold via in situ polymerization, which is a facile, cost-effective method. The hydrogel precursor solution is placed into the capillary mold and then cross-linked to form CHFs under different conditions, such as UV, thermal, physical interactions, etc. Generally, the materials of capillary molds are glass, silicone, polyvinyl chloride, polytetrafluoroethylene, and polydimethylsiloxane. Most capillary molds have tunable mechanical strength, elasticity, transparency, biocompatibility, and high fidelity of molding micro- and nano-structural features, which facilitate CHFs to detach from capillary mold. Here, some examples of CHFs fabricated via capillary polymerization technique are given.

Xu et al. injected the hydrogel precursor solution consisting of anhydrous calcium chloride, acrylamide (AM), N,N-methylenebisacrylamide (BAM), branched polyethylenimine (PEI), photoinitiator-2960, water and glycerol into a silicone tube with the inner diameter of 1 mm using a syringe (**Figure 4**a).[117] Subsequently, 3D cross-linking network structure CHF was formed by exposing the silicone tube to ultraviolet (UV) irradiation for 30 min, seeing that BAM as crosslinker contributed PAM chains to crosslink together via the strong covalent bond and branched PEI interacted synergistically with polyacrylamide (PAM) chains via hydrogen bonds. The fracture and recombination of the hydrogen bonds played a dominant role in dissipating energy and preventing crack propagation, thus imparting CHF with excellent stretchability. The diameters of original CHF could be tuned by further stretching, which can reach 100 times of their original length in the absence of breaking (Figure 4b). A single CHF was successfully collected by winding around a glass beaker and can be easily processed to hydrogel fiber web or spider web (Figure 4c). In addition, these CHFs demonstrated high conductivity (0.75 S m^{-1}), excellent anti-freezing performance (–40 °C), favorable weight retention ratio (≈90%), strong adhesiveness, sensitive strain sensing, and light guiding capability, which own great potential in the application for flexible functional electronics. Zhou et al. fabricated a highly-conductive PEDOT:PSS/PANI hybrid CHF for the high performance fiber supercapacitor via hydrothermal assembly of a commercial PEDOT:PSS dispersion followed by acid treatment and in situ chemical polymerization of aniline in a glass capillary with inner diameter of 0.5 mm.[90] The synergistic effect of highly-electroactive PANI and the robust PEDOT hydrogel framework endowed this hybrid CHF with high mechanical property, high specific capacitance and excellent rate capability.

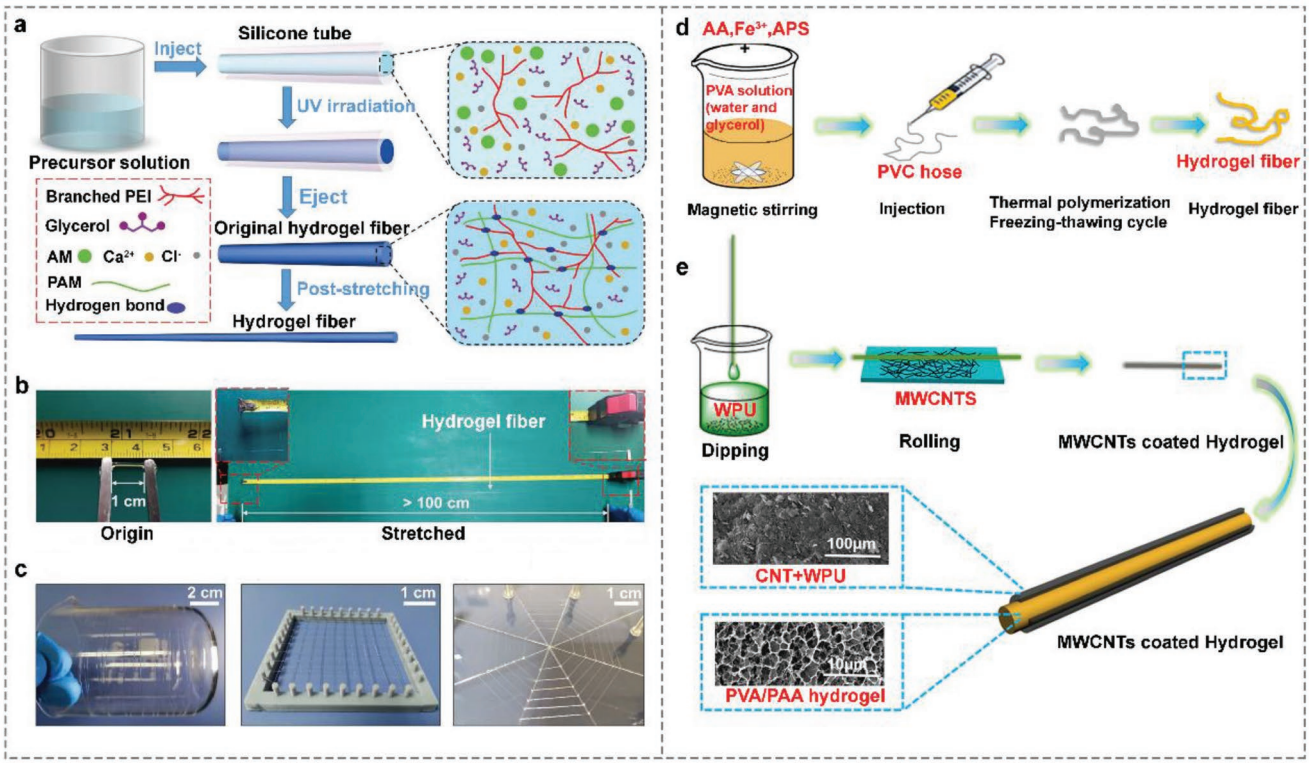

Figure 4. Schematic diagram of capillary polymerization method for fabricating CHFs. a) CHF was fabricated in a silicone tube. b,c) Photographs of CHFs in different states. Reproduced with permission.[117] Copyright 2021, Royal Society of Chemistry. d) The PVA/PAA hydrogel fiber was first fabricated in a PVC hose. e) The MWCNTS-PVA/PAA CHFs were produced by coating MWCNTs on the surface of PVA/PAA hydrogel fibers. Reproduced with permission.[118] Copyright 2020, Elsevier.

Corresponding to the above one-step process, another preparation strategy is two-step method that non-conductive hydrogel fibers were prepared first by employing capillary mold, which were further coated with the electrochemically active material through immersion to obtain CHFs. For instance, Wu et al. first constructed a non-conducive poly(vinyl alcohol)/poly (acrylic acid) (PVA/PAA) hydrogel fiber by means of the polymerization of PVA/AA monomer with a mixture of glycerol and water solution in PVC hose (Figure 4d), followed by coating multi-walled carbon nanotubes (MWCNTs) onto the surface of as-prepared PVA/PAA hydrogel fiber to produce an MWCNTS-PVA/PAA (C-PVA/PAA) CHF (Figure 4e).[118] The PVA chains significantly endowed PVA/PAA hydrogel fiber with a high tensile strength of 3.8 MPa and toughness of 13.7 MJ m^{-3}. Moreover, the presence of glycerol ensured PVA/PAA hydrogel fiber excellent flexibility and anti-freezing even at –15 °C. This C-PVA/PAA CHF had a high gauge factor of 25 at the strain of 40%, high stability and repeatability of 5000 cycles, and a fast response time of 225 ms. As a result, the C-PVA/PAA CHF could monitor large-scale and subtle body movements accurately and timely, exhibiting tremendous potential in the field of wearable sensing electronics for sports and health detection. Currently, a wide range of CHFs were designed and fabricated by capillary polymerization method, which is not only suitable for various crosslinking strategy and relatively broad range of materials, but also independent of the reaction rate of gelation whether it is fast and slow. The size, shape and diameters of CHFs was controlled by capillary mold. However, the inevitable pitfall is that it is difficult to realize continuous, large-scale industrial preparation of CHFs.

3.1.2. Draw Spinning

Another frequently used approach for fabrication of CHFs is draw spinning.[120–124] In nature, spiders spin silks by pulling the liquid proteins from different glands to form a gel mixture before spinning, which subsequently transforms into a solid fiber upon exiting the spider.[125,126] The mechanism of draw spinning is that the hydrogels were manually stretched to prepare CHFs with assistance of the entangle interactions of the molecular chains. Inspired by spider silk production mechanism, Zhao et al. reported a CHF via one-step stretching concentrated solution of ultra-high molecular weight sodium polyacrylate (PAAS) in a mixture of water and dimethyl sulfoxide based on the intertwining and hydrogen bonding interactions between PAAS polymer chains, which was further coated with a waterproof layer of polymethyl acrylate (PMA) to form a core–shell anti-freezing and stretchable PAAS-PMA CHF (**Figure 5**a).[94] This CHF composed of a conductive PAAS core and an insulating PMA cover demonstrated high tensile strength (5.6 MPa), large stretchability (1200%), fast resilience (<30 s) from large strain, high ionic conductivity (2 S m^{-1}), and low temperature resistance (–35 °C), which could be used

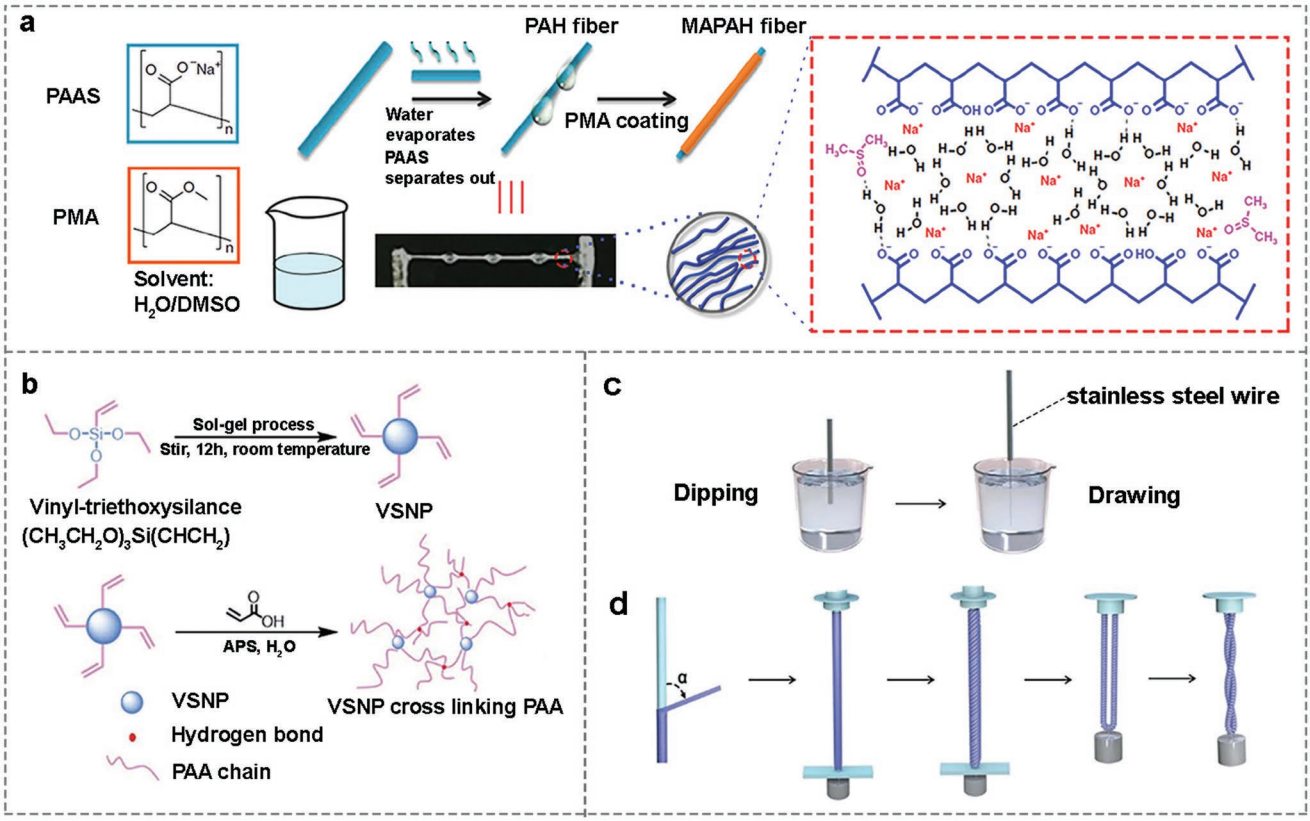

Figure 5. Schematic diagram of draw spinning for fabricating CHFs. a) The preparation process of PAH and core-shell MAPAH fibers due to the interwining and hydrogel bonding interactions between PAAS polymer chains. Reproduced with permission.[94] Copyright 2018, Springer Nature. b) Synthesis process of polyacrylic acid hydrogel cross-linked by vinyl-functionalized silica nanoparticles. c) Hydrogel fiber drawing process. d) Coating a thin layer of aligned carbon nanotube sheets on the surface of hydrogel fibers to form HF-ACNS$_x$. Reproduced with permission.[119] Copyright 2021, Royal Society of Chemistry.

in novel stretchable electronics. However, this non-covalently crosslinked CHF exhibited significant creep and hysteresis.

Another typical example, You et al. fabricated a kind of CHFs via draw spinning a polyacrylic acid bulk hydrogel cross-linked with viny-functionalized silica nanoparticles and followed by coating aligned carbon nanotube sheets (ACNSs) on its surface to obtain HF-ACNS CHFs (Figure 5b–d), which exhibited enhanced water tolerance, high mechanical strength with a breaking strength of 79 MPa and a breaking strain of 65.8%.[119] This as-prepared HF-ACNS CHF exhibited super contraction behavior, which could irreversibly contract upon exposure to water moisture. Hence, it could be applied as reversible fiber actuators demonstrating hydromorphic contractile actuation if the carbon nanotube alignment direction was parallel to the hydrogel fiber direction. This wonderful work plays an enlightening significance in designing and fabricating CHFs with high mechanical properties for highly responsive sensors. Chen et al. reported tough hybrid CHFs with heterogeneous networks via draw spinning clay/P(MEO_2MA-co-OEGMA-co-NIPAM) nanocomposite hydrogel, followed by in situ polymerization of aniline.[120] These CHFs demonstrated high conductivity of 87.99 S m^{-1}, high fracture energy of 172.43 kJ m^{-2}, excellent tensile strength of 7.21 MPa, and good swelling resistance due to their multimolecular interactions among the heterogeneous structured and intrinsic hydrophobic property of PANI. Benefiting from the knittability of gel fibers and piezoresistive performance of PANI nanostructure, they could serve as wearable sensors integrated into traditional fabrics to detect human motions and physiological signals. Draw spinning for preparing CHFs gets ride of dependence on the capillary mold. However, it is regrettable that this approach is still difficult to effectively fabricate uniform and continuous CHFs in a large scale. Moreover, draw spinning cannot also make the gelation process keep the same pace as the fiber forming process.

3.2. Continuous Fabrication Techniques

3.2.1. Wet Spinning

Currently, continuous fabrication techniques have been recognized as an important and mainstream directions to design and continuously prepare CHFs in large-scale production.[127–131] Among these techniques, classical and mature wet spinning is a versatile and efficient approach to construct fibrous materials, which has also been widely utilized to produce CHFs on a large scale on account of its existing maturity and controllability. The formation mechanism of CHFs is that the precursor solution is injected into a coagulation bath, followed by a non-solvent induced phase-separation process and covalently/non-covalently

cross-linked reaction simultaneously, which can successfully synchronize the fiber spinning and gelation process. A classic example is the fabrication of alginate hydrogel fiber, the solution of sodium alginate is injected into calcium chloride ($CaCl_2$) solution and subsequently crosslinked rapidly by exchanging of Na^+ and Ca^{2+} to form the fibrous hydrogel network.

Song et al. reported and manufactured a new type of conductive organohydrogel fibers on the basis of the combination of a meticulous designed hybrid crosslinking strategy composed of a physically and covalently hybrid crosslinking mechanism and a simple solvent replacement process.[127] The precursor solution containing alginate, an end-functionalized poly(ethylene glycol) prepolymer and photoinitiator-I2959 was spun into a coagulation bath containing Ca^{2+} under UV light via wet spinning, which can rapidly form ion-crosslinked nascent hydrogel fibers (**Figure 6**a), and subsequently replacing the water of the hydrogel fibers by glycerin to produce organohydrogel fibers in force (Figure 6b). The ion-crosslinked networks ensured the continuity of the spinning process and the covalently crosslinked networks endowed CHFs with excellent mechanical properties, which could be collected on a continuously winding drum spool (Figure 6c) and woven to a knitted textile (Figure 6d). Accordingly, these as-prepared organohydrogel fibers demonstrated high conductivity (0.765 S cm^{-1}), excellent anti-freezing property (<–80 °C), outstanding long-term stability (>5 months), transparency, stretchability (400% ± 9.6%), and negligible hysteresis during the cyclic loading and unloading, which can be applied as strain sensors for high-frequency (4 Hz) and high-speed (24 cm s^{-1}) motion of a simulated engine. Additionally, they were also favorable for wearable strain anisotropic sensors, optical fibers, data gloves, and flexible soft electrodes. Wang et al. prepared a smart ionogel fiber composed of thermoplastic polyurethane (TPU) and ionic liquid (IL) by the facile and scalable wet spinning.[85] The IL/TPU solution was injected into the coagulation bath to form IL/TPU ionogel fiber due to the DMF diffusion and the penetration of water into the IL/TPU filaments. The prepared IL/TPU ionogel fibers demonstrated good weavability and flexibility, and excellent stretchability (up to 700% strain) owing to the remarkable elasticity of TPU and vast hydrogen bonds between IL and TPU chains. It could serve as a wearable strain sensor with good linearity in an ultrawide sensing range (up to 700%), ultralow-detection limit (0.05%), fast response (173 ms) and recovery (120 ms), and high reproducibility to monitor both subtle physiological activities and large human motions.

The majority of needles of wet spinning is a single mode, and the multi-needles mode is conducive to construct versatile CHFs with promising application prospects. For example, Chen et al. fabricated a suite of core–shell segmental configuration multifunctional hybrid fibers via dual-core coaxial wet spinning (Figure 6e), consisting of a conductive reduced-graphene-oxide-doped poly(2-acrylamide-2-methyl-1-propanesulfonic acid-co-acrylamide (rGO-poly(AMPS-co-AAm)) hydrogel with strain-sensitive features (Figure 6f) and a thermochromic elastomer containing silicon rubber and thermochromic microcapsules with the thermosensitive features.[128] By means of accurately controlling the extrusion substance as a core layer, a conductive hydrogel precursor solution, or a thermochromic elastomer prepolymer, a core–shell segmental structure was smartly obtained. These multifunctional CHFs possessed numerous advantages involving good conductivity, high stretchability and excellent extrudability, which could be applied as wearable strain and temperature sensors for multi-aims based on different sensing mechanisms, such as monitoring human motion, detecting body/surrounding temperatures, and decorating colors. In summary, wet spinning combined with the various hybrid cross-linking strategies can provide an effective solution for the rational design and construction of CHFs as well as effectively ensure gelation of hydrogel and fiber formation simultaneously. The diameters of CHFs as small as tens of micrometers can be well controlled by the diameters of the needle and the rate of injection. More importantly, wet spinning is not only appropriate for continuous large-scale production of CHFs from industry to daily life, but also has a promising potential to design and fabricate multi-functions or multi-components flexible wearable devices such as transistors, sensors, displays, supercapacitors, and batteries.

3.2.2. Microfluidic Spinning

Microfluidic spinning can accurately manipulate micro-scale fluids with the assistance of microchannels controlled by precision-machined devices, which has achieved remarkable performance in biomedicine diagnosis, environmental monitoring, military science and aerospace fields due to its numerous advantages of small size, less sample consumption, fast detection speed, convenient operation, multi-functional integration, and high accuracy.[132–137] The difference of two spinning techniques is that there are two or more streams of coaxial flowing in microfluidic channels, among which the wet spinning is usually the single mode. Hence, microfluidic spinning has been widely adopted to design and produce CHFs at the micrometer scale owing to their considerable promising features and merits, which can precisely regulate their morphology, size, microstructure, chemical composition, and physical and chemical properties.[138–144] The formation mechanism of CHFs is as follows: first, the common precursor solution is injected into the inlet of a microfluidic chip, then delivered through microchannels in a laminar flow; second, precursor solution is directly extruded from the outlet of microchannels or embedded syringe needles or glass capillaries; finally, once extruded, precursor solution can be rapidly cross-linked or solidified based on various gelation methods including UV light, ionic or chemical cross-linking, and solvent exchange, leading to the formation of CHFs in a short period. In other words, the continuous fluid of the precursor solution is sheathed by a second solution and then generates continuous CHFs by solidifying the inner flow via crosslinking or solidification in the microchannels. As a classical case, Xu et al. made sodium alginate (SA) as the cortex spinning solution and $CaCl_2$ as the core spinning solution to form spiral-shaped alginate hydrogel fibers through an ionic cross-linking reaction in a coaxial microfluidic device.[138] However, this alginate hydrogel fiber crosslinked with weak ions bonds usually exhibited inferior mechanical strength.

To overcome this dilemma, functional nanomaterials and stimuli-responsive polymer networks can be generally integrated into CHFs to enhance the mechanical properties and

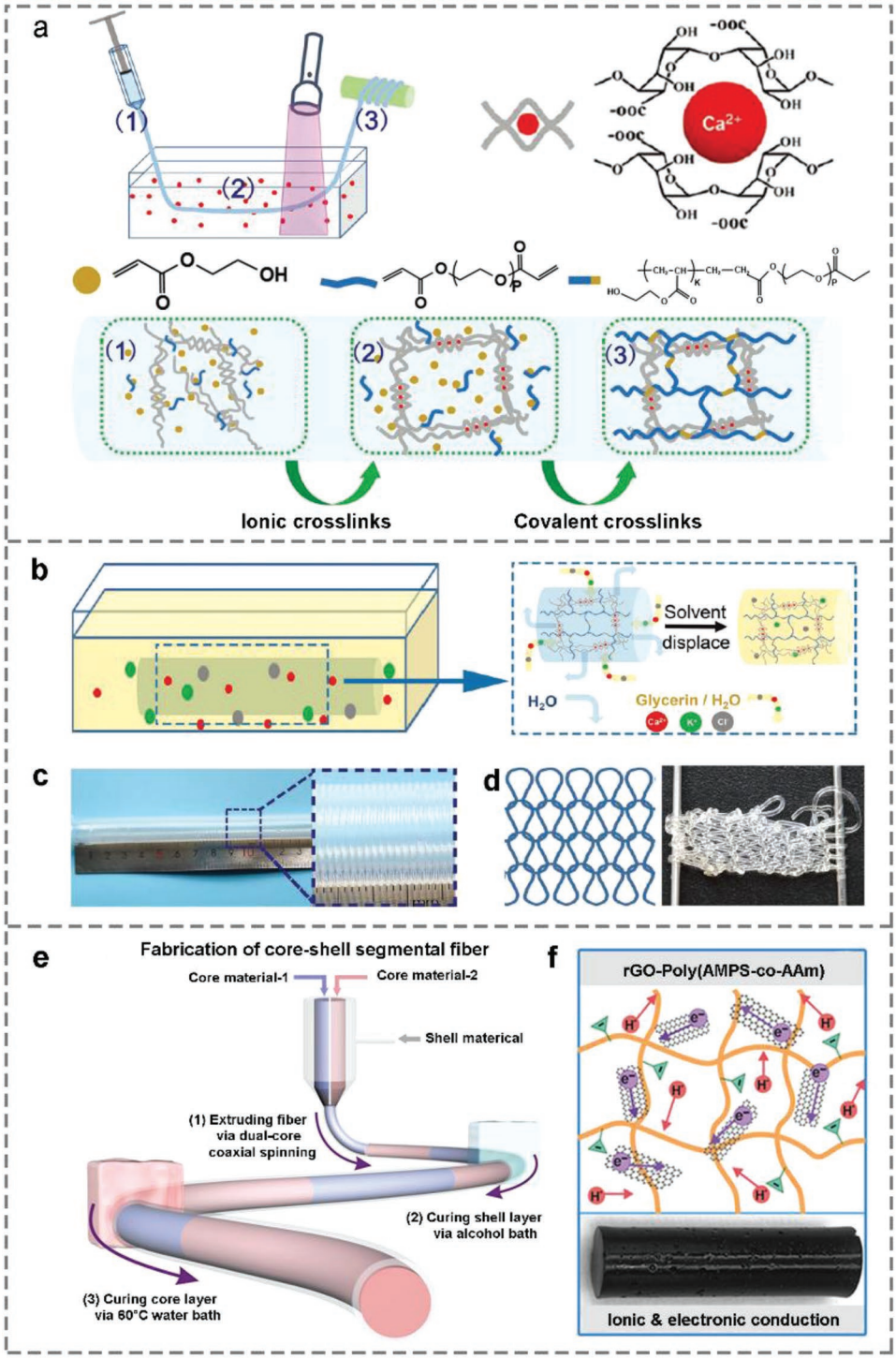

Figure 6. Schematic diagram of wet spinning for fabricating CHFs. a) The preparation process of CHFs via wet spinning based on ionic crosslinks and covalent crosslinks and b) organohydrogel fibers by solvent displacement. c) Photograph of a long single fiber and d) a knitted textile. Reproduced with permission.[127] Copyright 2020, Wiley–VCH. e) The fabrication of conductive hydrogel/thermochromic elastomer hybrid fibers with core–shell segmental configuration via dual-core coaxial wet spinning. f) The schematic conduction mechanisms and photos of rGO-Poly(AMPS-co-AAm) hydrogel as strain-sensitive materials. Reproduced with permission.[128] Copyright 2020, American Chemical Society.

multi-functionality of single-component CHFs. For instance, Peng et al. fabricated GO/PAM/SA nanocomposite CHFs based on alginate templating via taking the advantages of the combination of microfluidic spinning and free radical polymerization.[145] As shown in **Figure 7**a, a self-made coaxial laminar flow microfluidic device composed of two coaxially aligned

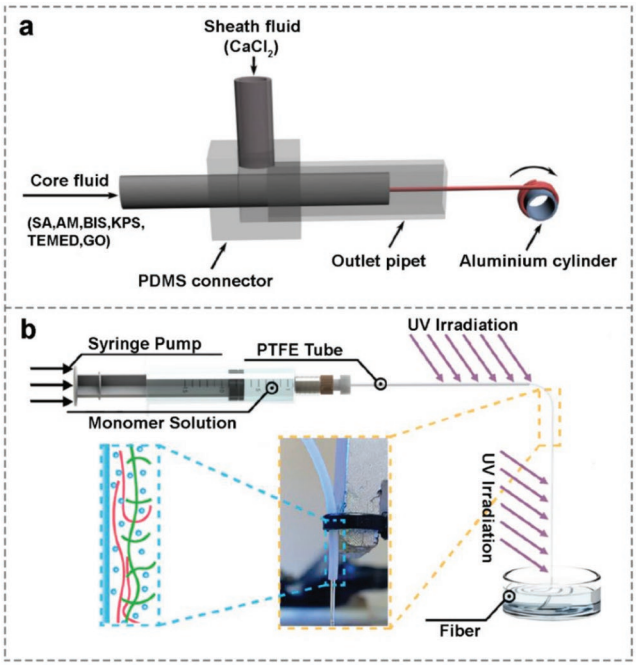

Figure 7. Schematic diagram of microfluidic spinning for fabricating CHFs. a) The GO/PAM/SA CHFs were fabricated via microfluidic spinning combined with free radical polymerization. Reproduced with permission.[145] Copyright 2018, Elsevier. b) The PAAM/PAMPS ionic CHFs were produced in microfluidic device based on the self-lubricated spinning strategy. Reproduced with permission.[146] Copyright 2020, American Chemical Society.

glass capillaries channels with different sizes was designed and assembled. The AM, SA, crosslinker, initiator, catalyst, and GO are used as the inner fluid, while $CaCl_2$ solution is sheath fluid. The continuous as-spun Ca-alginate-based CHFs could be produced rapidly via ion crosslinking reaction when Ca^{2+} in sheath fluid diffused into the core fluid. Subsequently, this as-spun fiber, served as a template, was put in soybean oil containing photoinitiator BDK for free radical polymerization and the crosslinking reaction of PAM. These GO/PAM/SA CHFs possessed high mechanical performance with fracture stress of 393 kPa and an elongation at break of 525%, excellent swelling characteristics and fast electro-responsive activities. Additionally, these CHFs can rapidly turn into a 90° bending angle within 45 s in 0.1 M Na_2SO_4 solution under the voltage of 20 V, which were expected to be adopted in artificial muscles, actuators and sensors.

Duan et al. developed electro-responsive PAAm/poly(2-acrylamide-2-methylpropanesulfonic acid) (PAAm/ PAMPS) ionic CHFs using a microfluidic device based on the self-developed self-lubricated spinning strategy. Specifically, the continuous fabrication of the CHFs was achieved via a two-step UV-initiated self-lubricated spinning approach (Figure 7b).[146] In the first place, a pre-gel solution containing AAm monomer and PAMPS lubricant was injected into a PTFE tube, and the AAm was partially polymerized through low-intensity UV radiating. Besides, the partially polymerized PAAm hydrogel fiber was pushed out of the PTFE tube under UV radiation continuously. Lastly, the researchers introduced triethylene glycol as a desiccant and plasticizer to exchange the water of CHFs via a simple immersing method to improve their mechanical property. The self-lubricated mechanism was that the PAMPS chains were expelled out of the PAAm networks with water molecules and the surface of the PTEF tube to generate the lubrication layer, which contributed to the continuous large-scale formation of CHFs. These CHFs with different diameters were easily achieved via adjusting the diameters of the PTFE tube rather than controlling the fluid speed. Moreover, they displayed outstanding mechanical flexibility with the maximum tensile strength of 5.6 MPa and maximum strain of 159%, which were easily customized into various complex geometries. More importantly, they could be applied as underwater soft robots to mimic multifarious biological motions, such as Mobula-like flapping, jellyfish-mimicking grabbing, sea worm-mimicking multi-degree of freedom movements, and human finger-like smart gesturing, which evidently surpasses over the majority of hydrogel fibers-based actuators reported previously.

Inspired by the spinning mechanism of spiders, Wei et al. constructed polyacrylamide-alginate CHFs in a large scale via a self-designed biomimetic microfluidic printer-head consisting of two coaxially aligned channels.[147] The shell layer liquid composed of the acrylamide monomer, the photoinitiator, the crosslinker and the alginate polymer; While the core layer liquid consisted of the accelerator for the polyacrylamide polymerization and the ionic crosslinker of alginate. Then the aforementioned shell layer liquid and the core layer liquid were directly mixed to form hydrogel with various configurations of microfibers, spider web, and 2D/3D tissue scaffolds. The mechanism of spinning and gelation was as follows. In the beginning, the partially solidified hydrogel fibers can be instantly fabricated via ionically crosslinked between Ca^{2+} and alginate polymer from the core and shell layers. Subsequently, these nascent hydrogel fibers were exposed to UV for covalently crosslinked polyacrylamide. Finally, various CHFs based materials were achieved via intertwining of covalently and ionically crosslinked networks. These CHFs could be used as sensors to detect human motions. Therefore, microfluidic spinning has broad potential in fabricating CHFs massively. Nevertheless, microfluidic spinning equipment is commonly expensive. Besides, only few materials can be suitable for microfluidic spinning, thus innovative materials still need to be developed for the popularity of microfluidic spinning.

3.2.3. 3D Printing

3D printing, also known as additive manufacturing, constructs customized implants and medical bioelectronics devices by "bottom-up" discrete-stacking method based on layer-by-layer deposition technique.[148–150] 3D printing, including fused deposition modeling, direct ink writing, inkjet printing, and stereolithography methods, has been successfully applied to fabricate various complex materials and provides significant opportunities for different types of materials and chemical/physical reactions. The resolution of 3D printing is generally in the micron scale, which is mostly used to construct biomaterial fiber scaffolds with precisely controlled the geometry and size. Moreover, the materials produced via 3D printing can better mimic

multi-level structures of natural tissues. Recently, hydrogels have been promising 3D printing raw materials to create fiber scaffolds with micro and sub-micrometer resolutions.[151–158]

Lei et al. developed an effective and feasible strategy to fabricate a 3D printed thermo-responsive, double network conductive hydrogel applied in a multifunctional skin-like sensor via a micellar-copolymerization method (**Figure 8**a).[157] The double network of this hydrogel comprised of physically crosslinked hydrophobic noctadecyl acrylate crystalline domains induced by sodium dodecylsulfate micelles and a covalent network induced by the chain transfer reaction in N,N-dimethylacrylamide polymerization. On the basis of a reversible physically crosslinked network, this hydrogel possessed a tunable rheological behavior with temperature responsiveness, that is, the viscosity of hydrogel decreased owing to the disentanglement of the physical crosslinks as the increase of the temperature, which was suitable for 3D printing technique to construct hydrogel fiber microstructures with a sub-millimeter resolution. For applications, a highly sensitive thermal or pressure stimuli skin-like capacitive sensor was assembled by integrating

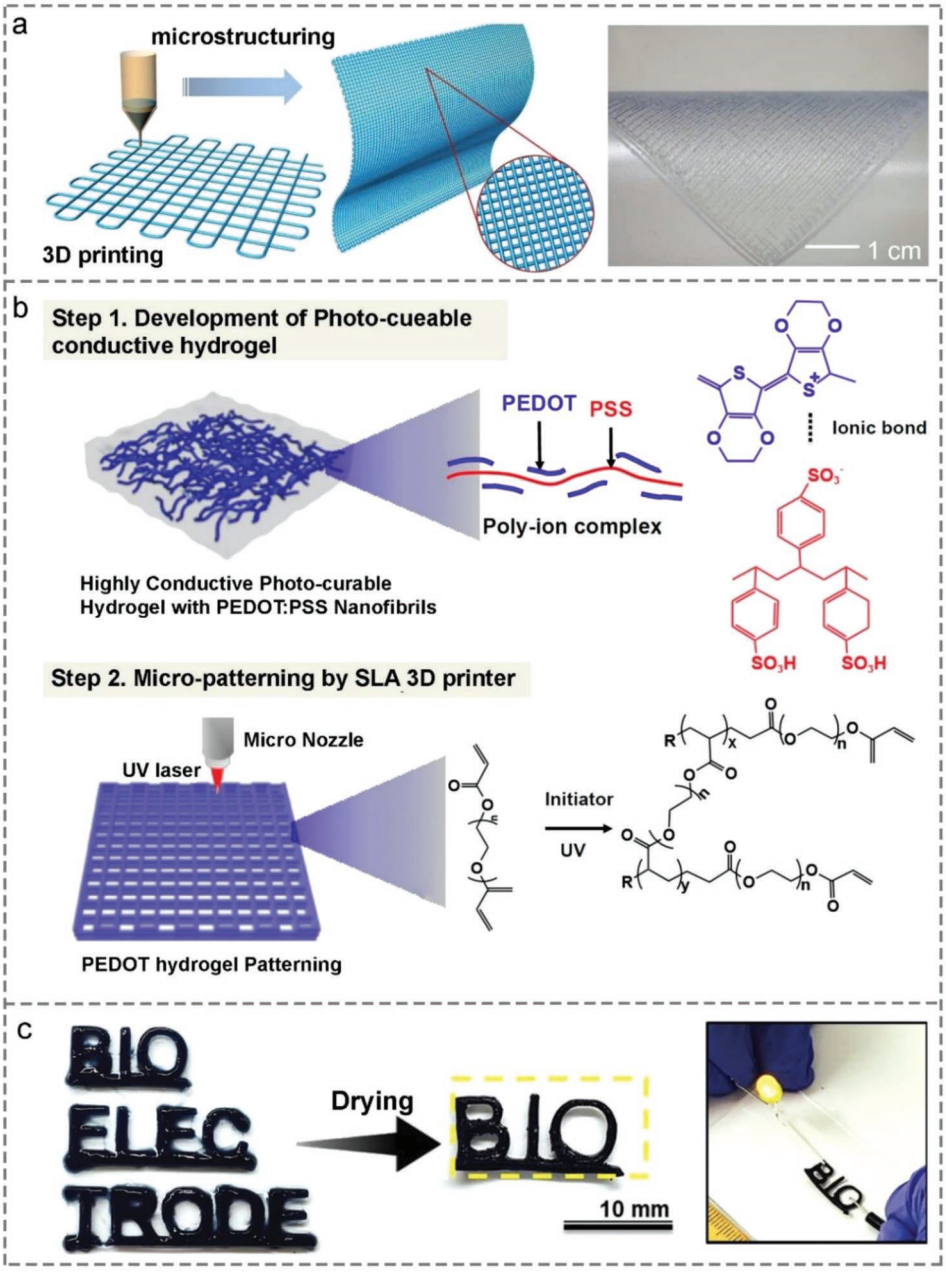

Figure 8. Schematic diagram of 3D printing for fabricating CHFs. a) Schematic illustration of 3D printing process and the grid microstructure of a printed hydrogel film. Reproduced with permission.[157] Copyright 2013, Royal Society of Chemistry. b) The preparation process of 3D PEDOT:PSS CHFs using SLA printing system. c) Optical images of PEDOT/PSS hydrogel in the swollen and dried states. Dried hydrogel was electrically connected to an LED lamp. Reproduced with permission.[158] Copyright 2019, Elsevier.

two grid-structured hydrogel films with a dielectric polyethylene layer, which could better sense body temperature, gentle finger touching, and finger bending motion. 3D printing provides a feasible and general strategy to fabricate the stimuli-responsive CHFs, which shows great potential in the future artificial intelligence, wearable devices, and human/machine interaction applications.

Heo et al. successfully utilized 3D printing equipped with a stereolithography system to print and pattern CHFs with various pre-designed architecture for the systematic delivery of electrical stimulation for enhanced neural differentiation (Figure 8b).[158] First, a photocrosslinkable and printable conductive hydrogel containing various concentrations of PEDOT:PSS from 0.00% to 0.91% was developed and characterized for printability. Second, the computer-aided design based architectural models with square pores were pre-designed with various CHFs spacing of 500, 600, and 800 μm before patterning. Then, the conductive printing solution composed of PEGDA, PEDOT:PSS, and photoinitiator was printed for fabrication of 3D structures with optimal conductivity for embedding of live cells using a 3D printer platform with *X*–*Y*–*Z* controlled UV laser system. Optical images showed that the hydrogel structures were composed of parallel-aligned hydrogel fibers with orthogonal orientation. Additionally, an image of the letters "bio electrode" was patterned using these printable conductive hydrogels with excellent conductivity, which could light an LED light successfully (Figure 8c).

Zhu et al. reported tough physical polyion complex (PIC) hydrogel fibers via 3D printing without any post-chemical reaction based on the sol–gel transition of PIC.[159] PIC solution composed of poly(3-(methacryloylamino)-propyl-trimethylammonium chloride) (PMPTC) and poly(sodium pstyrenesulfonate) (PNaSS) was extruded directly into deionized (DI) water to form PIC hydrogel fibers owing to the enhancement of ionic bonding between PMPTC and PNaSS. Moreover, the proper gelation speed and dynamic nature of ionic bonds also facilitated the interfacial bonding between different gel fibers, guaranteeing the integrity and toughness of printed gels. The printed PIC hydrogels showed excellent mechanical properties in terms of extensibility, strength, and toughness. The 3D printing technology based on sol–gel transition provided a facile approach to fabricate tough CHFs with complex structures. Although 3D printing can effectively prepare various CHFs and process them into complex and delicate 3D structure patterns with pre-designed geometrical shape, the instruments are complex and high cost. The development of suitable biomaterials for printing is a major challenge at present. On one hand, materials with both biocompatibility and shear thinning rheological properties limited the development of 3D printing tissue engineering scaffolds. On the other hand, the addition of fillers in CHFs may significantly affect their printability and conductivity.

3.2.4. Electrospinning

In the past few decades, electrospinning has been a quite important method to fabricate nanofiber materials.[160–162] The working mechanism of electrospinning is as follows: the spinning solution is first pumped out by a syringe pump or pressured gas into the tip of a needle (e.g., spinneret) connected to a high direct current voltage source. The solution initially forms a hemisphere drop due to the surface tension, which can be charged and elongated into a solution jet under the increasing high-voltage power and subsequently directed toward the grounded collector. According to the type of collector, nanofibers are deposited to obtain a fibrous mat with a random or preferential arrangement. Benefiting from these advantages of electrospun nanofibers with small size, high porosity, large specific surface area, and easy functionalization and modification, electrospinning is also widely applied to construct various CHFs.[163–166] Generally, there are two approaches to form CHFs. One way is post-electrospinning, the nanofiber membrane fabricated via electrospinning is handled with UV light or heating to initiate the cross-linking reaction of CHFs. Another way is reactive electrospinning, the spinning solution containing the polymer and cross-linker forms the crosslinking networks of CHFs during the electrospinning process. In addition, hydrogels can also be severed as a spinning solution or create core-shell composite microfibers by associating with a previously fabricated synthetic fibrous mat.

Zhou et al. designed and fabricated sandwich-structured hybrid hydrogel nanofibers composed of two layers of aramid nanofibers (ANFs) reinforced polyvinyl alcohol (PVA) hydrogel fibers mat via electrospinning and interlayer of AgNWs/PVA composite via vacuum-assisted filtration (**Figure 9**a).[52] First, the ANF-PVA fiber mats were fabricated via electrospinning. Second, sandwich-structured ANF-PVA/AgNWs hybrid fiber mats were prepared by vacuum filtration deposition of AgNWs/PVA suspension on the surface of ANF-PVA fiber mats and followed by coated layer of ANF-PVA fiber mats via electrospinning in sequence. Finally, ANF-PVA/AgNWs hybrid hydrogel fiber mats were obtained by immersing in DI water. The synergistic formation mechanism of these CHFs were attributed to the physical crosslinking sites of the PVA crystalline structure and strong hydrogen bonding interactions between the PVA hydroxyl groups and carbonyl groups in ANF polymer chains. They demonstrated high tensile strength of 5.5 MPa, modulus of 15.4 MPa, and toughness of 5.7 kJ m^{-2} owing to the strong hydrogen bonding interactions between PVA and ANFs molecular chains, the improved crystalline structure of PVA, the reinforcement of ANFs as well as in-plane aligned nanofibrous structure. The conductivity of these CHFs reached 1.66×10^4 S m^{-1} and could be easily tuned by changing the contents of AgNWs. Additionally, they exhibited very stable, strain-invariant conductivity under different complex deformation ascribed to the strong interfacial interactions between the ANF-PVA and AgNWs/PVA layers, as well as the mesh-like conductive network of AgNWs. Therefore, they not only were applied as excellent flexible EMI shielding materials, but also as electrochromic materials fabricated through Joule heating driven by a low voltage of <1.5 V. This work discovers a novel strategy to fabricate CHFs with outstanding mechanical properties and excellent conductivity simultaneously, which shows great potential in flexible bioelectronics. Wang et al. reported a core-shell scaffold based on aligned conductive nanofiber yarns (NFYs) within the hydrogel fibers.[167] The aligned NFYs composed of polycaprolactone, silk fibroin, and carbon nanotubes

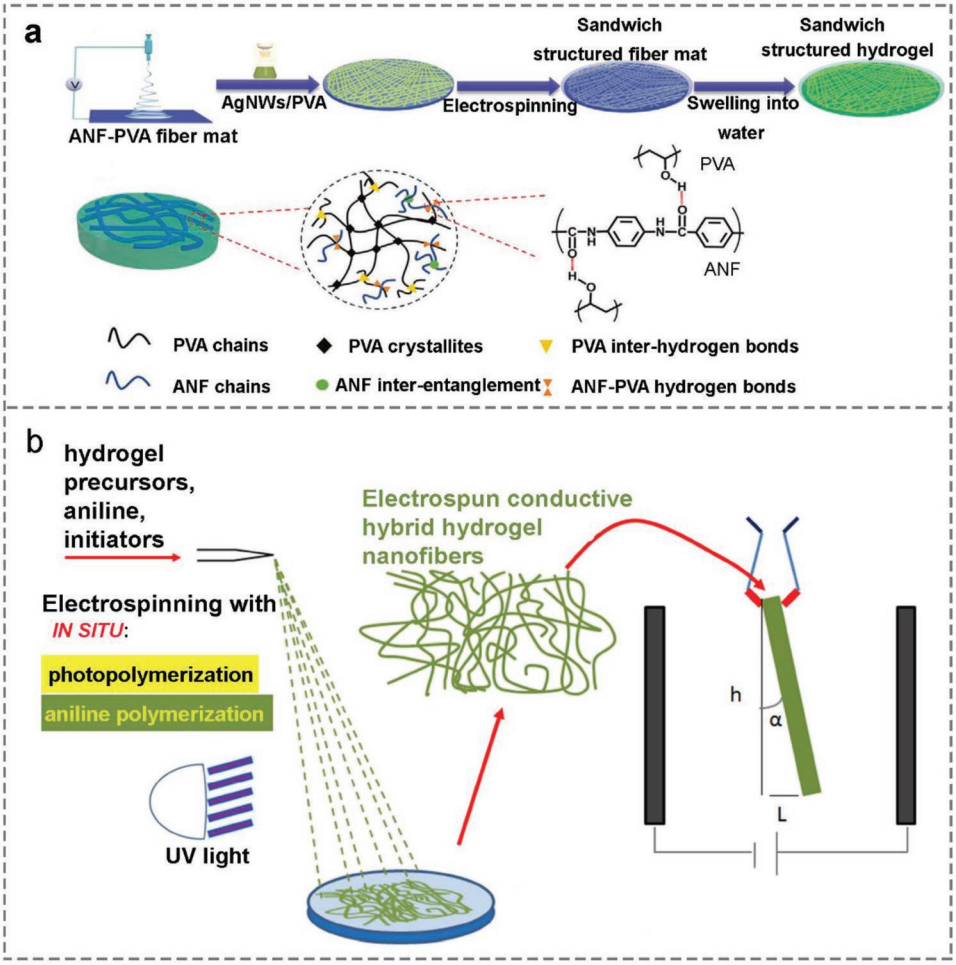

Figure 9. Schematic diagram of electrospinning for fabricating CHFs. a) The fabrication procedure and the molecular interactions of ANF-PVA/AgNWs hybrid hydrogel fiber mat via electrospinning combined with vacuum-assisted filtration. Reproduced with permission.[52] Copyright 2021, Wiley–VCH. b) The preparation process of electrospun hybrid hydrogel fiber mat by reactive electrospinning with in situ synthesis of conjugated polymers for actuators. Reproduced with permission.[168] Copyright 2020, Elsevier.

were prepared by a developed dry-wet electrospinning, then 3D core-shell scaffolds were fabricated by encapsulating NFYs within the hydrogel shell after the photocrosslinking reaction, which were able to control the cellular alignment and elongation of nerve cells in this 3D environment.

Miranda et al. reported electrospun hybrid hydrogel nanofiber mats via combining reactive electrospinning with in situ photopolymerization of the hydrogel precursor solution and polymerization of aniline (Figure 9b).[168] The electrospinning solution was the mixture solution of hydrogel precursor solution composed of AA, AAM, PEGDA, photoinitiator, and PVA and the conjugated polymer precursor solution of aniline. The role of PVA made the viscosity of the solution large enough for electrospinning. This electrospun hybrid hydrogel fiber mat was formed simultaneously as the UV radical photopolymerization of hydrogel precursor solution and aniline polymerization. It displayed excellent electrical conductivity of 0.01 S cm^{-1} and outstanding mechanical properties with an elastic modulus of 10 MPa due to the presence of PANI, shorter diffusion path lengths and higher interfacial areas of the nanostructured system, which could be applied as a high performance electroactive actuator. The conductive hydrogel fiber mats are promising for a wide range of applications due to their ease of fabrication, lack of residual monomer, high porosity, and excellent mechanical properties. However, electrospinning merely produces nonwoven fiber mats, strictly speaking, which are not real hydrogel fibers. Moreover, the residual organic solvent of hydrogel fibers are not friendly to the environment and humans. Finally, the advantages and disadvantages of six fabrication techniques of CHFs are summarized in **Table 2**.

4. Applications

Conductive fibers are indispensable parts of flexible electronics, especially smart electronic textiles. Traditional conductive fiber materials with low stretchability, including carbon fibers (CNT fibers, reduced GO fibers), metal-coated fibers, polymer fibers and composite fibers materials, extensively hinder their development and application.[147,169–171] CHFs possess significant benefits in terms of unique 1D linear structure, high aspect ratio, excellent mechanical flexibility, and knittability, which have a

Table 2. Advantages and disadvantages of fabrication techniques of CHFs.

Fabrication techniques	Advantages	Disadvantages	Reference
Capillary polymerization method	Facile, cost-effective, intuitive, suitable for various crosslinking strategies and materials	Time-consuming process, limited length, difficult to realize continuous, large-scale industrial preparation	[90,117,118]
Draw spinning	Facile, low-cost, prepared CHFs with ordered polymer chain alignment	Fail to fabricate uniform and continuous CHFs	[94,119,120]
Wet spinning	Versatile, synchronize the fiber spinning and gelation process, appropriate for continuous large-scale production of multi-functional CHFs	Need coagulation bath, complex post-treatment process	[85,127,128]
Microfluidic spinning	Production of meter-long CHFs in a relatively short time, precisely regulate the morphology, size, microstructure, and physical and chemical properties of CHFs	Expensive apparatus, not suitable to create complex architecture, few available materials	[145–147]
3D printing	Effective, micro and sub-micrometer resolutions, fabricate various complex, and delicate 3D structures	Expensive and complex apparatus, limited materials with sufficient rheological properties	[157–159]
Electrospinning	Ease of fabrication, fabricated CHFs with high porosity and excellent mechanical properties	Most are nonwoven fiber mats, toxicity of the solvents	[52,167,168]

great prospects in flexible electronics, such as energy harvesting devices, energy storage devices, smart sensors, and biomedical electronics. Furthermore, various textile techniques have been integrated into CHFs for flexible wearable electronics.

4.1. Flexible Energy Devices

4.1.1. Flexible Energy Harvesting Devices

Energy harvesting devices collect and convert various forms of energy into electrical energy.[173–177] Converting thermal and mechanical energy from the body as well as solar energy to electricity energy has been considered a promising way to harvest energy. Based on the coupling of triboelectric and electrostatic induction effects, triboelectric nanogenerators (TENGs) are commonly used as energy harvesting devices, which convert mechanical motion in the surrounding environment into electrical energy. TENGs have been extensively employed in biomedicine, chemical, and electronic fields due to their massive merits of high energy conversion efficiency, low cost, and the possibility of using a variety of materials. CHFs with excellent stretchability and high conductivity are much more suitable as electrode materials for TENGs, which demonstrate promising applications and market value in the field of energy harvesting.[172,178–182]

A case in point was that Shuai et al. ingeniously constructed physically cross-linked poly (NAGA-co-AAm) (PNA) CHFs with excellent stretchability and self-healing property via combining dry-wet spinning and the principle of reversible thermally sol-gel transition (**Figure 10**a).[55] These PNA CHFs exhibited high tensile strength of 2.27 MPa, excellent stretchability of 900%, outstanding conductivity of 0.69 S m^{-1} and self-healing capability. Finally, coating elastomer PMA thin layer to PNA CHFs to fabricate core-shell structure PNA/PMA CHFs, which effectively reduced the water evaporation and absorption of PNA CHFs. These PNA/PMA CHFs were woven into triboelectric nanogenerator fabrics successfully converting mechanical motion energy into electrical energy (Figure 10b,c). The output open-circuit voltage (V_{oc}), the transferred charge quantity (Q_{sc}), and pulsed AC short-circuit current (I_{sc}) of this triboelectric nanogenerator can reach −36 V, 10 nC, and 0.7 µA, respectively (Figure 10d). They were expected to be utilized in next-generation multi-functional smart textiles and wearable electronics.

Except for TENGs as effective means to harvest energy above, thermoelectric (TE) materials can also be applied as another important medium for energy harvesting, which have the ability to convert heat into electricity at a small temperature gradient between human body and the ambient. Liu et al. manufactured PEDOT:PSS CHFs with TE property in a poly(tetrafluoroethylene) capillary mold based on the gelation mechanism of π–π stacking interaction and hydrophobic attraction between PEDOT chains of PEDOT:PSS solution induced via concentrated H_2SO_4 (Figure 10e).[172] The PEDOT:PSS CHFs immersed in DI water were too brittle to keep the fiber shape. Therefore, the solvent of EtOH, acetone, or IPA as coagulation bath was introduced to replace DI water to retain the structural integrity of PEDOT:PSS CHFs. Furthermore, these PEDOT:PSS CHFs post-treated with ethylene glycol (EG) and dimethyl sulfoxide (DMSO) exhibited the highest conductivity of 172.5 S cm^{-1} and only 5% decrease in seebeck coefficient, and a higher TE performance. Finally, five pairs of p-type PEDOT:PSS CHFs and n-type CNTs fibers were connected in series to construct a p–n-type TE fiber device (Figure 10f), which demonstrated a satisfactory output voltage of 20.69 mV and a significant power density of 481.17 µW cm^{-2} under the temperature difference of 60 K (Figure 10f). This work not only provides a guiding approach for fabricating PEDOT:PSS CHFs with high conductivity and excellent TE performance, but also for the development of organic TE fibers for wearable energy harvesting devices.

4.1.2. Flexible Energy Storage Devices

Energy storage devices are also fundamental parts of wearable and portable electronics.[183,184] In recent years, fiber-shaped supercapacitors have become the most promising flexible energy storage devices due to their substantial advantages, such as lightweight, high power density, excellent cycle stability, high safety, flexible, and knittability.[185–188] Conductive hydrogel systems can improve the active area of electroactive materials, optimize transport channels of electrons and ions and enhance the

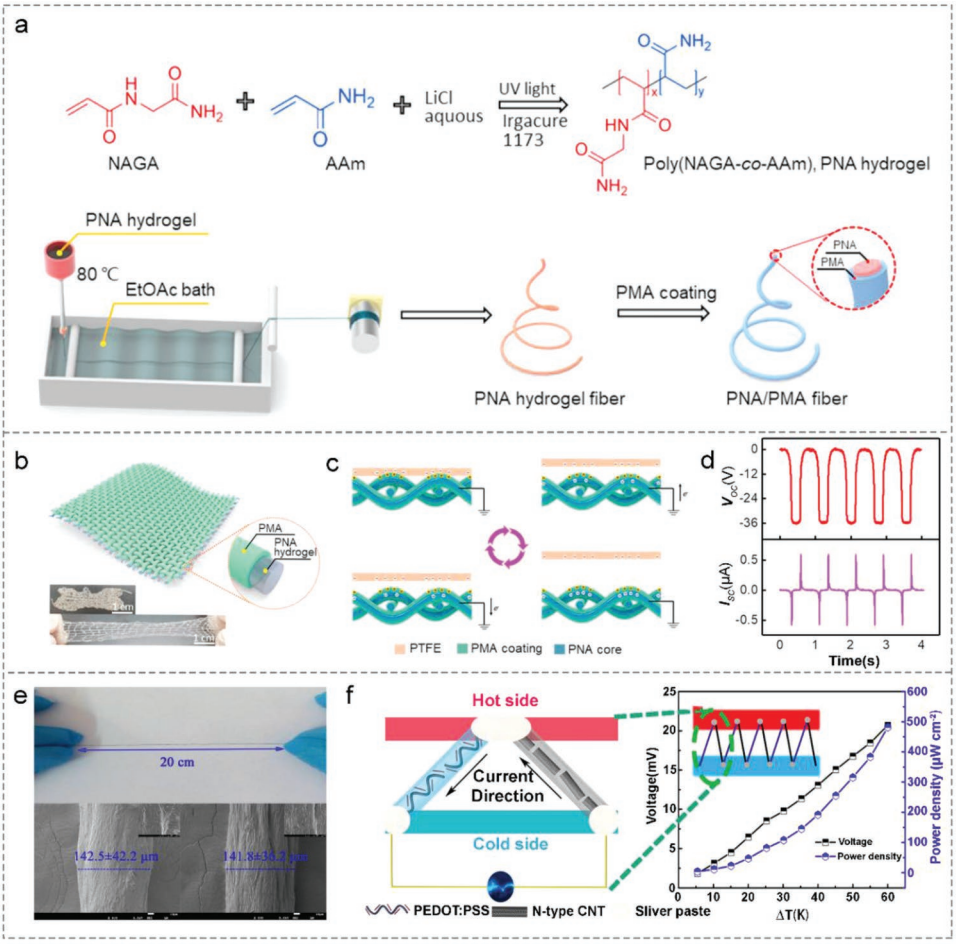

Figure 10. CHFs-based energy harvesting devices. a) The preparation procedures of PNA hydrogel, PNA CHFs, and core-sheath PNA/PMA CHFs. b) The schematic diagram, c) mechanism, and d) performance results of a TENG textile woven from PNA/PMA CHFs. Reproduced with permission.[55] Copyright 2020, Elsevier. e) The photos and SEM images of PEDOT:PSS CHFs. f) The schematic diagram and performance results for TE device based on five pairs p-type PEDOT:PSS CHFs and n-type CNT fibers. Reproduced with permission.[172] Copyright 2018, American Chemical Society.

solid-liquid interface of electrodes and electrolytes via adjusting and controlling of morphologies, structures, composition, and interface properties of hydrogels or constructing various nanocomposite strategies using synergistic effect of different materials and nanostructures. More importantly, the nanocomposites as high performance electrode materials will boost their specific capacitance, rate capability, and cycling stability.[76,185–189] Therefore, CHFs with outstanding electrochemical activity, relatively high conductivity, and exceptional mechanical flexibility show extensively application in the energy storage field.

For instance, Li et al. fabricated 3D self-supporting and interconnected PANI/RGO CHFs via supramolecular self-assembly architectural strategy and one-step chemical oxidative polymerization in capillary glass tubes (**Figure 11**a).[89] The unique combination of 2D RGO nanosheets and 3D PANI network crosslinked by phytic acid (PA) molecule based on strong intermolecular forces consisting of π–π stacking, electrostatic and hydrogen bonding interactions among PANI, PA, and GO (Figure 11b), which were constructive to reduce the obvious aggregation in the following reduction process. As a result, this PANI/RGO hydrogel could not only be easily and successfully molded into fibers without any aggregation, but also demonstrated uniform interconnectivity, excellent conductivity, and enhanced mechanical properties. A stretchable all-gel-state fiber supercapacitor assembled using two similar PANI/RGO CHFs electrodes and PVA/H_2SO_4 hydrogel showed a high volumetric energy density of 8.80 mWh cm^{-3} at a volumetric power density of 30.77 mW cm^{-3}, which was superior to other fiber supercapacitors previously reported. The cyclic voltammetry (CV) changes of this fiber supercapacitor in normal, knotted, and twisted states were almost invisible, which demonstrated an outstanding flexibility and robustness for practical applications (Figure 11c,d). Moreover, it could be remolded into a spring-like structure with excellent elasticity and shape-memorability (Figure 11e).The design philosophy of all-gel-state fiber supercapacitors provided novel way for powering next-generation wearable and portable electronics.

In actual production and daily life, low temperature environment will deteriorate the electrochemical performance and service life of energy powering devices. Consequently, designing frost-resistant conductive hydrogels can better adapt to extremely cold climate change and effectively broaden the

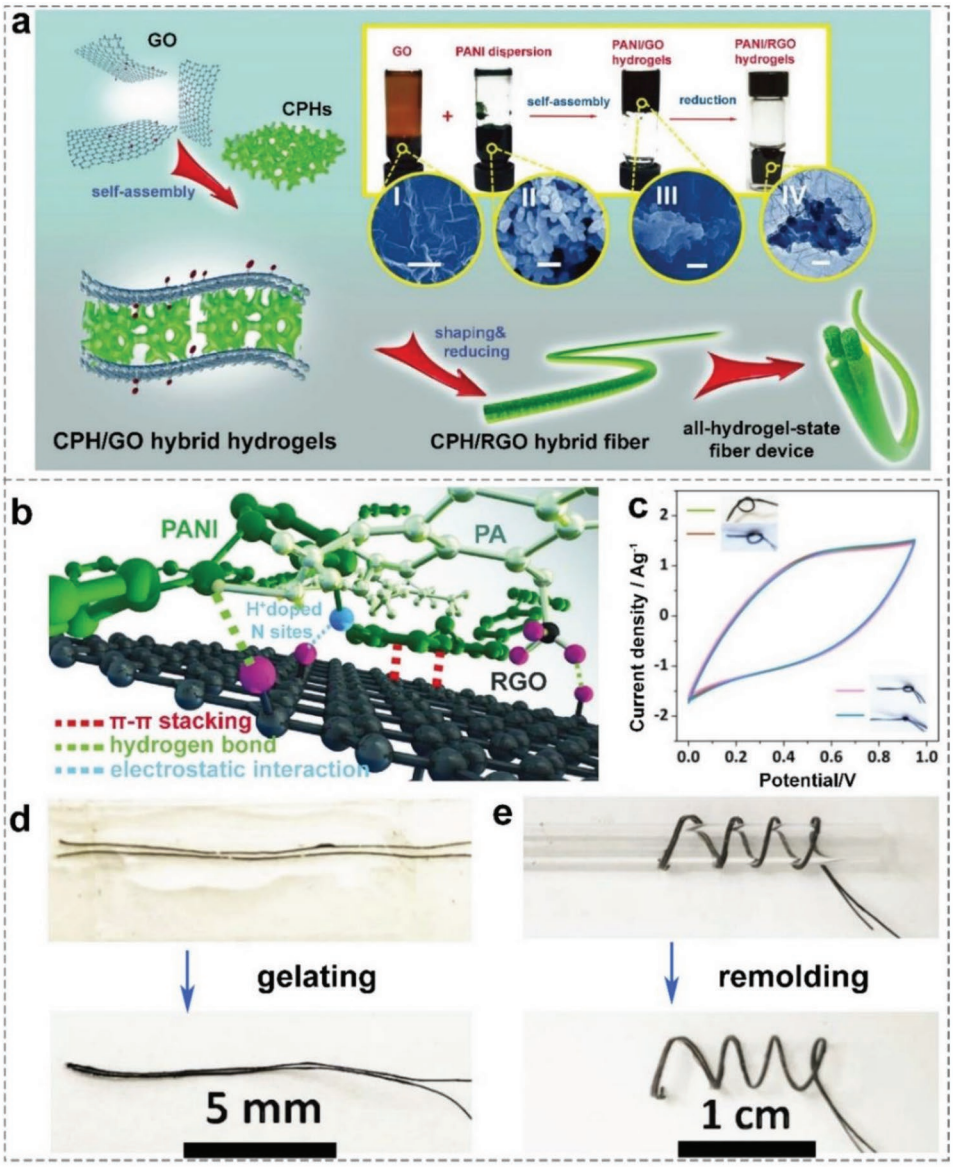

Figure 11. a) The formation diagram of PANI/GO CHFs. b) The possible interactions among PANI, PA, and RGO. c) Assembly process of a fiber supercapacitor and d) its CVs curves in normal, curved, and twisted states. e) Assembly process of a spring-like full gel state device. Reproduced with permission.[89] Copyright 2018, Wiley–VCH.

operating temperature of energy powering devices. Xu et al. manufactured highly stretchable, anti-freezing double network RGO/PEDOT:PSS/PVA (GP-PVA) CHFs via a one-step hydrothermal self-assembly strategy followed by solvent replacement (**Figure 12**a).[91] The resultant GP-PVA CHFs achieved great conductivity of 182 S m^{-1}, a high specific capacitance of 356.1 F g^{-1} at 0.6 A g^{-1} for a single electrode in 1 M H_2SO_4 solution and excellent flexibility even at −30 °C on account of their ordered structures, smooth ion transport channels and anti-freezing PVA crosslinked networks. An all-gel-state fiber supercapacitor assembled by integrating GP-PVA CHFs electrodes with the anti-freezing PVA/H_2SO_4 gel electrolytes exhibited outstanding frost resistance, high capacitance, and excellent flexibility. This anti-freezing device possessed a high specific capacitance of 281.2 F g^{-1} at 25 °C and maintained a high specific capacitance of 212.6 F g^{-1} at −20 °C (Figure 12b). Additionally, it also demonstrated the excellent capacitance retention of 91% after 5000 charge and discharge cycles at −20 °C (Figure 12c). Finally, a highly stretchable spring-like supercapacitor exhibited excellent capacitance retention of 92% after 5000 stretching cycles at a high strain of 500%. This innovative work provided a good reference to develop anti-freezing fiber-based energy storage devices.

In practical application scenarios, flexible electronics are generally subjected to various external mechanical stress, which greatly decrease the stability, security and lifespan of the devices. In order to overcome these difficulties, endowing the devices with self-healing property can effectively maintain their structural integrity, enhance their durability and functionality, and reserve their mechanical and electrochemical stability, which makes

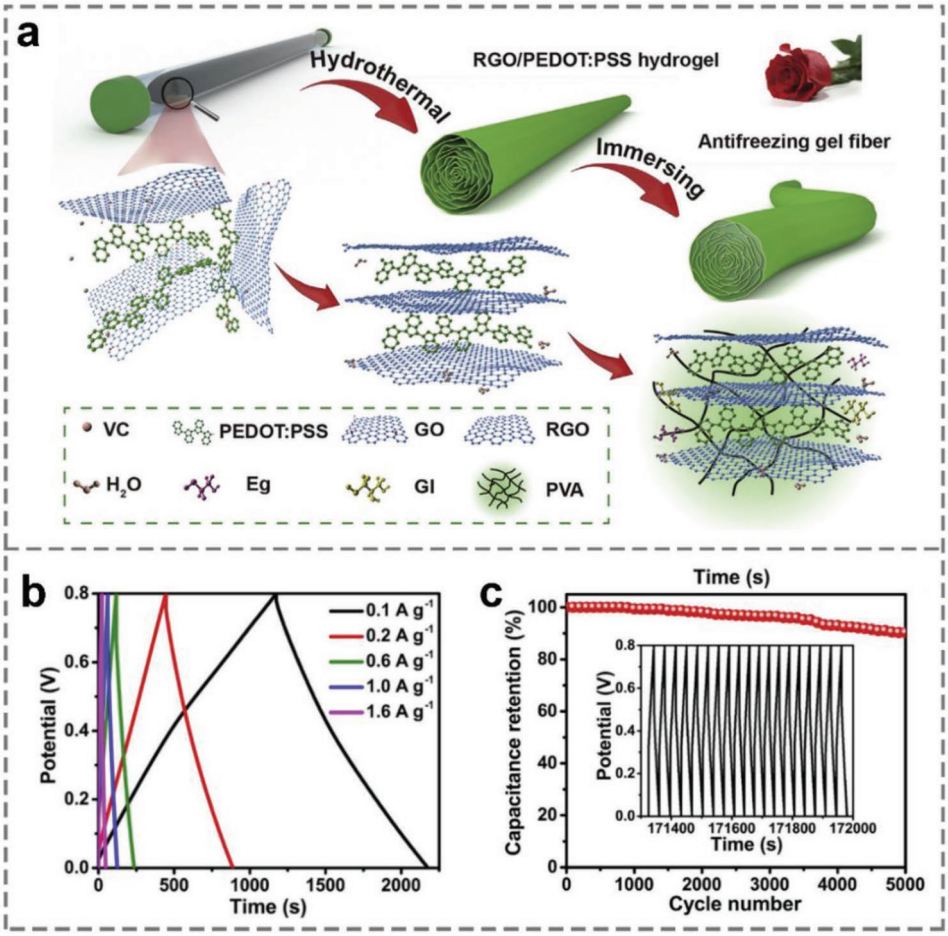

Figure 12. a) The preparation diagram of anti-freezing GP-PVA CHFs. b) GCD profiles and c) cycle life of the antifreezing supercapacitor at −20 °C. Reproduced with permission.[91] Copyright 2020, Elsevier.

wearable devices better meet the requirement of the complex and changeable mechanical environment. Jia et al. constructed urchin-like $NiCo_2O_4$ nanomaterial-based polyvinyl alcohol/potassium hydroxide (PVA/KOH) CHFs using a traditional coating route.[190] First, high-molecular-weight PVA/KOH hydrogel fibers were fabricated in a silicone capillary pipe via freezing and thawing technique. The as-prepared PVA/KOH hydrogel fibers possessed great stretchability of 300% at a tensile stress of 12.51 kPa, excellent ionic conductivity, and outstanding self-healing ability. Subsequently, urchin-like $NiCO_2O_4$ nanomaterials were synthesized by a hydrothermal reaction and were brushed onto the PVA/KOH hydrogel fibers at a stretching state. Finally, the low-molecular-weight PVA/KOH electrolytes were coated on the surface of $NiCO_2O_4$/PVA/KOH CHFs. A novel stretchable, self-healing fiber supercapacitor was fabricated via enwinding two identical $NiCO_2O_4$/PVA/KOH CHFs electrodes, which showed high areal specific capacitance of 3.88 mF cm^{-2} at a current density of 0.053 mA cm^{-2} and an excellent capacitance retention rate of 88.23% after 1000 charge and discharge cycles. Moreover, this fiber device exhibited excellent self-healing performance with a capacitance retention rate of 82.19% after four cuts/self-healing. This work paved a new way for wire-like self-healing supercapacitors and further extended the lifetime of flexible electronics.

4.2. Flexible Smart Sensors

4.2.1. Strain Sensors

In recent years, flexible smart sensors can effectively collect information from the human body and the surrounding environment in an intelligent, friendly and real-time manner, occupying an increasingly important position in the fields of wearable devices, health care and military defense.[191,192] CHFs with unique biocompatibility, interfacial adhesion, stretchability, and conductivity can quickly withstand, sense and convert external environmental stimulus into electrical signals and be used to build highly sensitive flexible strain/stress or temperature sensors for wearable electronics.[96,147,193–195] CHFs are ideal candidates for wearable strain sensors to monitor human motion.

Ju et al. reported highly stretchable, good water-retaining, and coating-free poly(acrylamide-co-sodium acrylate)/Fe^{3+} (P(AAm-co-AA)/Fe(III)) CHFs via a redox-active Fe-citrate complex regulation for continuously draw spinning strategy (**Figure 13**a).[96] They had great stretchability of 500% and a high elastic modulus of 0.27 MPa thanks to the ingenious energy dissipation mechanism of the dynamic and

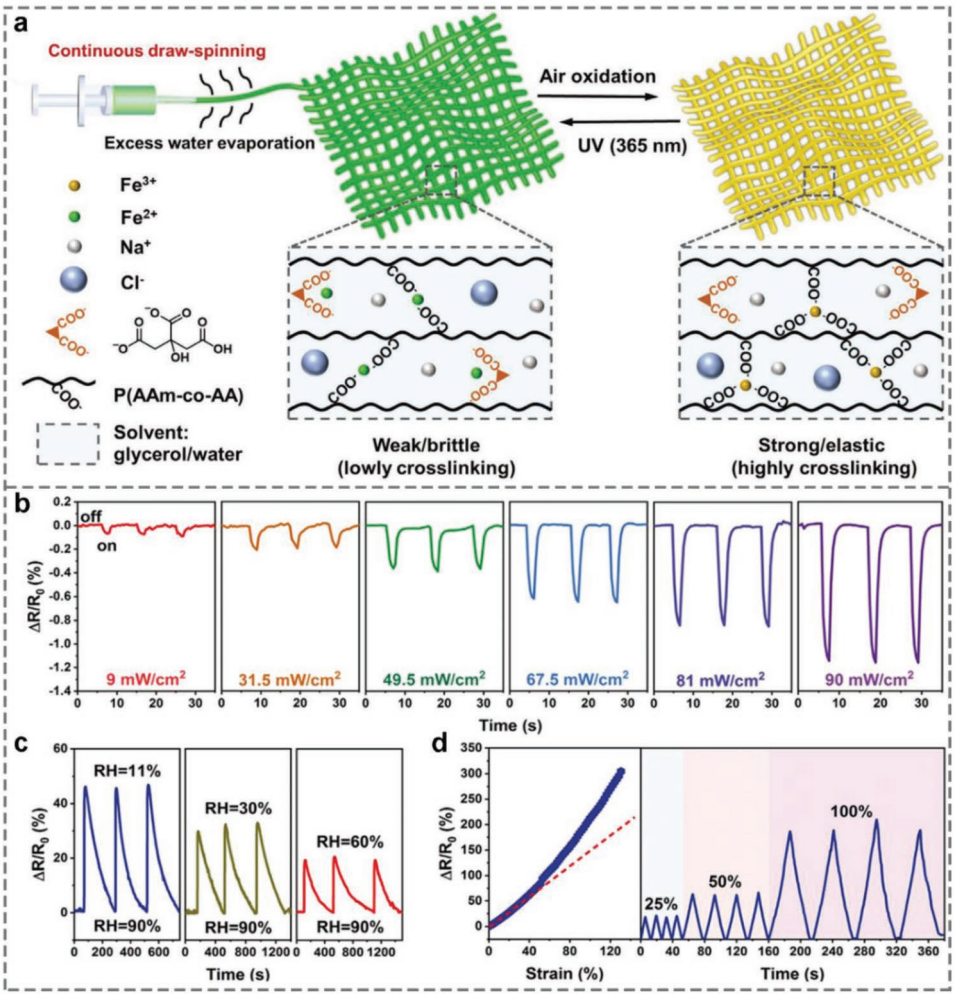

Figure 13. a) Fabrication diagram of P(AAm-co-PAA)/Fe(III) CHFs via draw spinning. b–d) The sensing properties of UV, humidity, and tensile strain of hydrogel microfiber net. Reproduced with permission.[96] Copyright 2020, Wiley–VCH.

recoverable coordination between Fe(III) and the carboxylate groups of polymer chains. Moreover, they exhibited remarkable frost resistance with a freezing point of –61 °C, water retaining feature, good elasticity even at –40 °C, and high ionic conductivity of 4.2 mS m^{-1}. Furthermore, CHFs possessed highly sensitive to various environmental stimulus of UV light, humidity and strain (Figure 13b–d), whose stiffness could be accurately controlled by humidity and UV light. This work not only presented a novel draw spinning strategy on the basis of the ancient redox chemistry of Fe-citrate complex with a well balance of spinnability and strength of CHFs, but also opened more avenues for designing and producing coating-free CHFs for intelligent electronics applications.

Wei et al. self-designed a biomimetic microfluidic printerhead consisting of two coaxially aligned channels for continuous construction of polyacrylamide-alginate CHFs in a large scale.[147] These continuous, uniform, and tough CHFs presented extraordinary stretchability (2100%) owing to the perfect energy dissipation mechanism of the reversible alginate network crosslinked by Ca^{2+} and short diffusion path between the calcium sources and alginate phases endowed by core-shell structure. The initial resistance of un-stretched CHFs was measured to 0.67 Ω m in 0.1 M KCl solution, which could be used as wires for lighting up LED bulbs. A printer super-robust web was applied as a sensor to accurately detect the minor and major body movement of the human elbow, implying that there was a shaper variation of the resistance when the elbow is repeatedly moved from 0° to 45°, 90°, and 135° (**Figure 14**). This work opened up new ways to shape tough hydrogels into designed 1D, 2D, and 3D structures with large scalability and robustness, which showed a wide range of potential applications for sensitive flexible electronics, tissue engineering and human-robot interfaces.

4.2.2. Temperature Sensors

Apart from strain/stress sensor, the human motions and health status can also be monitored via CHFs capturing body temperature in real-time, which is an important signal to evaluate fever, inflammation, and wound infection of the human body. Regarding temperature sensing, the most common

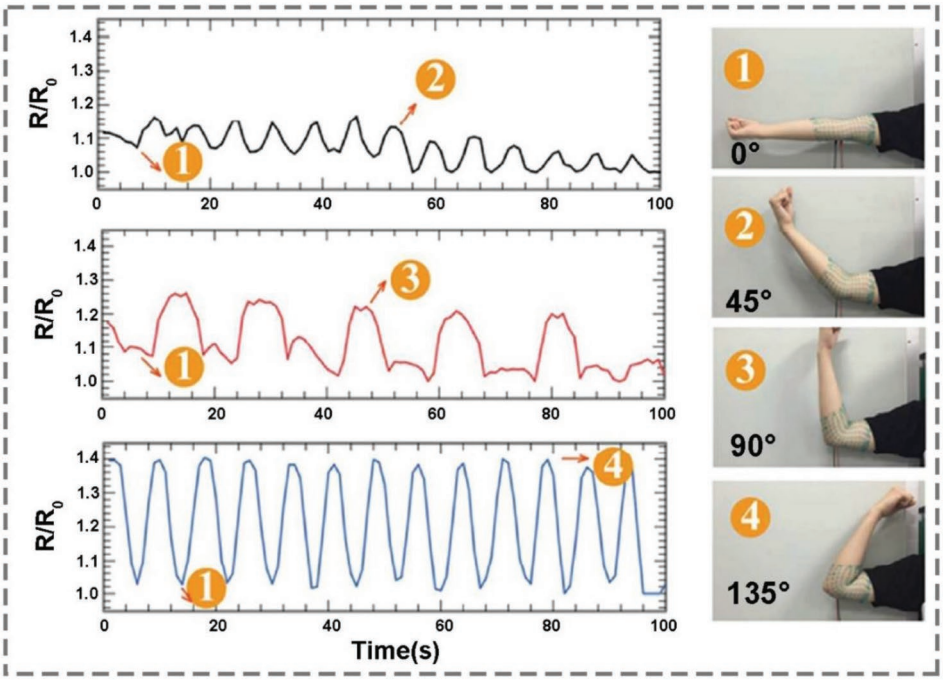

Figure 14. The printed web could be used as sensor to detect human motions, as the elbow was subjected to repeated bending and relaxing from 0° to 45°, 90°, and 135°, respectively. Reproduced with permission.[147] Copyright 2018, American Chemical Society.

mechanisms of CHFs rely on the color changes of the materials. Various temperature sensitive particles composed of colorant, developer, and solvent were introduced to the hydrogel systems. The combination and destruction of colorant and developer was caused as the temperature changes, a color composite was formed owing to the developer taking electrons from the colorant in low temperature while the color was faded owing to the developer taking electrons from the solvent as high temperature. For example, wang et al. reported a high porosity, strength, and conductivity hydroxyethyl cellulose-polyvinyl alcohol (HEC-PVA) composite hydrogel via employing the freezing and thawing cycles to handle the mixture solution of HEC and PVA.[193] The gelation mechanism was that HEC and PVA underwent a lot of hydrogen bonds, which could not only reduce PVA micro-crystalline regions, but also increase the number and size of the pores, thus increasing the conductivity of hydrogels. The HEC-PVA hydrogel demonstrated a high ionic conductivity of 5.77 S m^{-1} and excellent mechanical strength of 2.86 MPa at the strain of 400.30%. The mechanical properties and ionic conductivity of HEC-PVA were easily tunable by adjusting HEC concentrations and the types of ions. Additionally, PVA-HEC organic hydrogel (PHOH) fabricated by introducing glycerin had high mechanical strength and conductivity even at −30 and 65 °C in harsh environments. On the basis of the above investigations and the requirements of miniaturization and intelligence of flexible electronics, the researchers incorporated various temperature sensitive particles into the initial reaction mixture to construct a high mechanical strength, ionic conductivity and temperature-sensitive woven organic hydrogel fiber in a polyvinyl chloride capillary tube. These temperature sensitive particles with different reversible colors that change with temperature (blue, red and green discolor at 28, 35, and 45 °C, respectively) could be widely applied to monitor the human–machine movement and temperature in different ranges. This work provided a novel fiber temperature sensor, which could promote the integration, miniaturization, and intelligence of wearable electronics.

4.3. Flexible Biomedical Electronics

4.3.1. Flexible Bioelectronics

CHFs as extracellular matrix analogues have excellent biological surface and interface compatibility, which can be considered as an ideal candidate to connect human tissues.[104] They are ideal carriers for the interaction and fusion of the human body and various electronics. Currently, CHFs have excellent application prospects in the fields of flexible biomedical electronics, such as organic electrochemical transistors (OECTs), flexible robots, tissue engineering, and biological detection devices.[196]

Zhang et al. fabricated injectable and healable PEDOT:PSS CHFs by injecting mixed precursor solution of PEDOT:PSS liquid and 4-dodecylbenzenesulfonic acid (DBSA) surfactant into a confined cylinder plastic tube based on the room-temperature gelation property of PEDOT:PSS free of any cross-linking agent and extra operations.[197] The as-prepared RT-PEDOT:PSS CHFs with excellent mechanical properties retained structural integrity when extruded from the cylinder tube via pressurizing. They could be processed into various shapes through the syringe by simply hand-writing, whose diameters could be tuned in different sizes of plastic tubes. The PEDOT:PSS CHFs were typical examples of electroactive

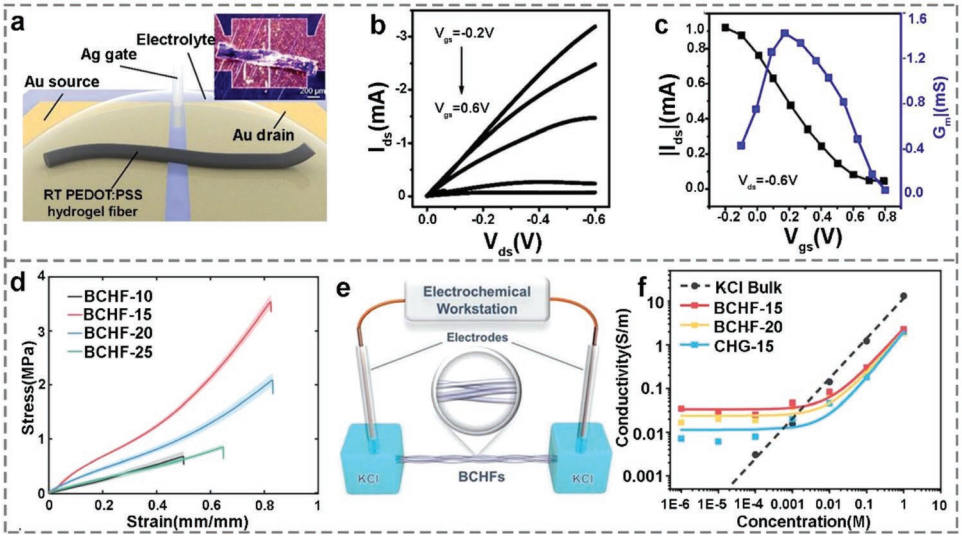

Figure 15. CHFs-based flexible bioelectronics. a) The schematic of OECTs based on RT-PEDOT:PSS CHFs. b) The output and c) transfer curves of the OECTs with RT-PEDOT:PSS hydrogel fibers as the channel. Reproduced with permission.[197] Copyright 2018, Springer. d) The tensile stress–strain curves of BCHFs. e,f) The schematic diagram of the ionic conductivity measurement of CHFs as nanofluidic devices. Reproduced with permission.[198] Copyright 2021, Royal Society of Chemistry.

materials for bioelectronics applications, OECTs were fabricated via simply syringe-injecting RT-PEDOT:PSS CHFs between two metallic electrodes (**Figure 15**a). The OECTs with a typical transistor behavior working in the depletion mode showed a maximum transconductance of ≈1.4 mS (V_{ds} = −0.6 and V_{gs} = −0.2 V) (Figure 15b,c). Hence, these PEDOT:PSS CHFs with good electrochemical properties will greatly promote their application and development in the field of soft flexible bioelectronics.

Zhang et al. continuously fabricated pure natural bacterial cellulose hydrogel fibers (BCHFs) via a facile continuous large-scale production wet pinning strategy free of any additional cross-linking step.[198] These pure natural bacterial cellulose-based ionically CHFs demonstrated a superior tensile strength of 3.74 MPa and high water content of 87% (Figure 15d). They could also retain 90% of their original strength even after being soaked in water for 14 days, which showed no swelling properties. Both the unique nanofibers network self-reinforced structures and non-swelling properties of these CHFs endowed them with wonderful stability of mechanical and volume properties even at high water content of 90%. Besides, the abundant nanochannels of CHFs were conducive to ion transport even at lower concentrations, which exhibited excellent bio-ion conductivity of 0.56 S m^{-1} in SBF simulated body fluid (Figure 15e–f). Meanwhile, they had satisfactory light-guiding capability with attenuation of 5.1 dB for guiding light at a wavelength of 515 nm. Integrated with good bio-ion conductivity and light-guiding capability, they could be directly used as high precision, a pure natural nanofluidic device without packaging for the detection of trace neurotransmitters in nerves, such as trace dopamine. This work not only provided a new and facile strategy to design and fabricate multifunctional CHFs, but also blazed a new trail for the development of next-generation biological multifunctional neural interfaces.

4.3.2. Tissue Engineering

Similar to the extracellular matrix of biological tissues, CHFs have excellent biocompatibility and are promising candidates for the next generation of bioelectronics interfaces, which are widely used in tissue engineering.

Mirani et al. developed a novel, cost-effective, and straightforward biofabrication method to continuously construct multitudinous multifunctional grooved solid and hollow hydrogel fibers with controlled fiber properties including morphology, cross-sectional shapes, porosity, material composition, and groove size via wet spinning.[199] Importantly, conductive GO and rhodium nanowires could be incorporated into the grooved hydrogel fibers system to produce CHFs, which tremendously extending their applications to tissue engineering, wound healing, smart drug delivery, wearable or implantable medical devices, and soft robotics. Additionally, the cellular alignment of various cell types including myoblasts, cardiomyocytes, cardiac fibroblasts, and glioma cells on these hydrogel fibers was evaluated, which were shown to induce controlled myogenic differentiation and morphological changes, depending on their groove size, in C2C12 myoblasts (**Figure 16**a). These CHFs could be processed into various complex 3D structure scaffolds via simple wet spinning, which show great potential in biomedical field. Heo et al. reported 3D printable PEDOT:PSS CHFs for neural tissue engineering.[158] Dorsal root ganglion (DRG) neuronal cells were encapsulated in gelatin methacryloyl (GelMA) hydrogels, and subsequently embedded in the 3D printed CHFs structure with different pore sizes in order to evaluate their cell viability and cytotoxicity via live/dead assay. Most encapsulated DRGs retained excellent cell viability with horizontal and vertical after 1 day of culture confirmed by confocal microscopic, which indicated that these CHFs had no significant cytotoxicity toward DRGs. Then, the DRG cell-encapsulated GelMA hydrogels were integrated with 3D printed conductive structure to evaluate

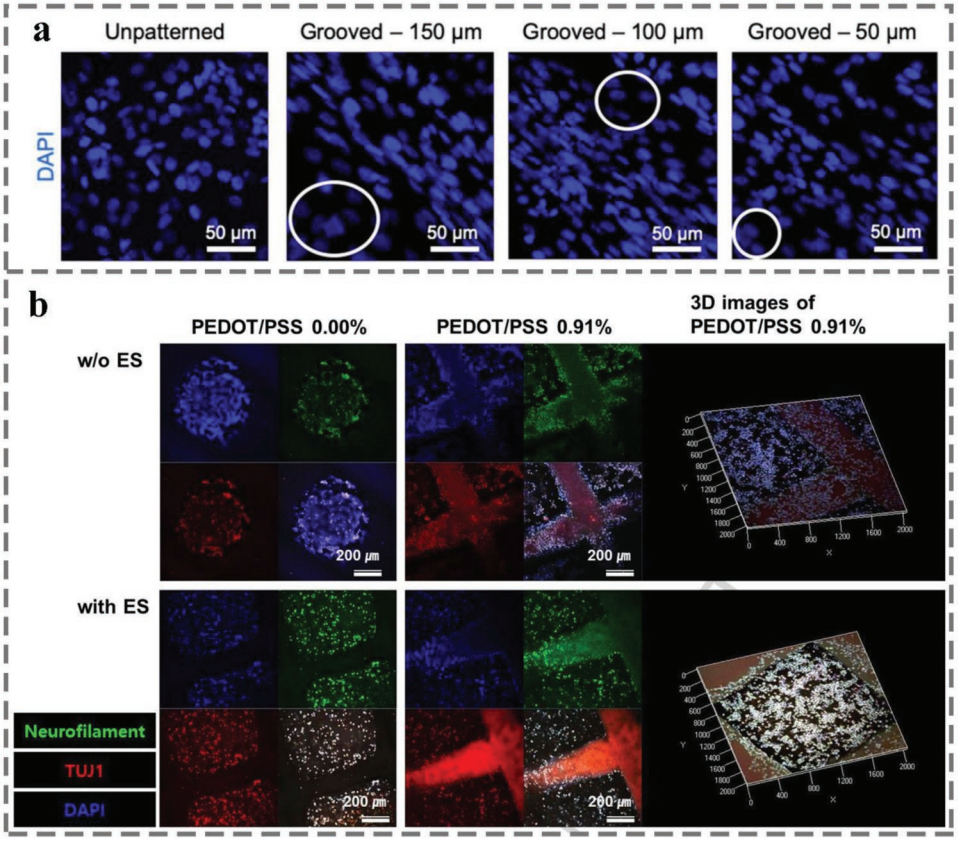

Figure 16. a) Grooved fibers direct C2C12 cells to unidirectional orientation and myogenic differentiation. Reproduced with permission.[199] Copyright 2018, American Chemical Society. b) Immunofluorescence images of encapsulated DRG cells in GelMA with 3D printed PEDOT/PSS hydrogels. Reproduced with permission.[158] Copyright 2019, Elsevier.

the efficiency of neural differentiation by electrical stimulation (ES) treatment. After 24 h of differentiation, 3D printed conductive hydrogel structures with PEDOT:PSS of 0.91% showed enhanced neuronal differentiation with a significant difference in neuronal gene expression with ES treatment (Figure 16b). Therefore, these CHFs could be useful in a wide variety of biomedical applications, such as biological signal recording devices, stimulation electrode, drug delivery devices, neural differentiation culture systems, and neural tissue regeneration.

5. Conclusion

Over the past decades, CHFs have drawn considerable attention in the realm of flexible electronics owing to their striking merits of hierarchically porous microstructure, high surface area, high conductivity, tunable physical and chemical properties, excellent interfacial biocompatibility, and large length-to-diameter ratio, outstanding mechanical flexibility, and knittability. The recent advances in the design, fabrication, and application of CHFs and manufacturing technology of flexible electronics have tremendously promoted the development of CHFs for flexible electronics. In this review, we first introduce the architectural features and function characteristics of CHFs. Subsequently, a variety of fabrication strategies including discontinuous and continuous spinning techniques of CHFs as well as their advantages and disadvantages are described comprehensively. Third, the applications of CHFs for flexible electronics are summarized in detail, such as flexible energy harvesting devices, flexible storage devices, flexible smart sensors, and flexible biomedical electronics.

In spite of substantially achieved progress, the development of CHFs in flexible electronic systems is still in its fledgeless stage, which is far from satisfying the requirements of commercialization on a large scale. The large gap between the laboratory and practical applications for the fabrication of CHFs still remain.

Primarily, the water evaporation of CHFs is an existing problem in the state of working conditions for flexible electronics. On one hand, CHFs spun in the air is prone to undergo severe dehydration. Even though some studies reported that dehydration could enhance the fiber strength and stretchability to a certain extent, it inevitably weakened the conductivity of CHFs because of the poor movement of ions. Consequently, the balance of strength and ionic conductivity of CHFs dependent on water content is extremely urgent to be established. On the other hand, the water in CHFs inevitably encounters to be frozen at subzero temperatures and dry at high temperature, inevitably limiting their practical applications in harsh environment. By reason of the foregoing, the presence of water produced by evaporation in CHFs contaminates the circuits as well as takes the edge off their mechanical properties and

conductivity, leading to serious performance degradation or even loss of basic functions of devices. To circumvent this challenge, the most popular strategy is to package CHFs with water-resistant elastomers. Nonetheless, the presence of elastomers coating layer may cause CHFs insensitive to environmental changes and increase the weight of devices, which is unconducive to the performance of the whole devices. Therefore, the development of an effective and facile strategy for designing and fabricating of CHFs with good water retention capacity, high conductivity, preferable temperature tolerance, and stable mechanical properties is a critical point to conquer in further.

Second, as the advancement of people living standard, pursuing of intellectualization and humanness, lightweight, miniaturizing and multifunctional electronics with maximizing performance have become the mainstream direction of the future technological innovations. As a result, designing and fabricating lightweight, miniature and multifunctional CHFs based flexible electronics is the key to well fulfill the demand of the public. For one thing, there is a growing trend to develop flexible electronics with new functions, such as stimuli-responsive properties (light, heat, chemicals, pH, and strain/stress), self-healing properties, shape memory properties, anti-freezing properties, enhanced biocompatibility and so forth, which can extensively expand the applications of CHFs for smart flexible electronics. To address this challenge, the collaborative composite strategy is an effective way to confer the multifunctional materials via introducing a variety of components with unique features, which might potentially bring the advantages of multi-components into full play, reducing the disadvantages of single component to the minimum at the same time. There is no doubt that the presence of synergistic effect between multiple components can drastically boost the performance of CHFs. However, to design the interactions between multi-components and optimize their complex interfaces issue (interfacial compatibility, interfacial strength, and stability) as the major challenges facing the development of multifunctional flexible electronics need to be studied in-depth. For another thing, the integration of electronic units with different functions including energy generators, energy storage devices, smart sensors, data collecting units, and feedback systems in one platform can efficiently promote the development of flexible, wearable, and portable electronics, serving as an emerging hot area for the applications of smart electronics. Intelligent, multifunctional, high matching, and compatibility of the human-machine interface are the future development directions of CHFs-based flexible electronics.

Third, although plenty of mature spinning techniques for fabricating CHFs have been developed, the fabrication of CHFs with high conductivity and high mechanical strength simultaneously remains a challenge. Additionally, an insight into the formation mechanism of CHFs is necessary to be sufficiently exploited. From the perspective of the novel construction strategy of a cross-linking network of hydrogels and processing strategy of spinning, the selection of spinning techniques, novel materials for hydrogel matrixes and electro-active compositions, as well as the synergistic interactions of different components, are fundamental to the design and fabricate CHFs with both conductivity and mechanical properties. In terms of the compatibility of crosslinking reaction rate and spinning process, it is urgent to develop more ingenious strategy to make slow polymerization reactions in accord with the rapid spinning process. It is the reason that crosslinking reaction is generally a time-consuming process under a stress-free state, and the spinning is a dynamic process under the drafting force. Therefore, it remains a challenge to explore new crosslinking strategies that match the spinning process to efficiently produce CHFs with reduced resistance and increased mechanical strength.

Furthermore, devising a facile and well-controlled method for fabricating and precisely tailoring the microstructures and properties of CHFs is the premise of its industrialization. Designing a variety of intermolecular interactions of materials to realize the deep integration between CHFs-based devices and the human body is the further direction in this field. Meanwhile, the balance of the functionality, stability and cost of CHFs-based flexible electronics will play an important role in the development of next-generation flexible electronics. The breakthrough in these research will provide useful guidance for large-scale industrialization of CHFs-based flexible electronics. It is anticipated that our future nanoworld would be lit up under the joint efforts and meaningful cooperation of engineers from different backgrounds and scientists from multidisciplinary fields such as chemistry, physics, engineering, biology, nanotechnology, and materials science.

Acknowledgements

W.L. and J.L. contributed equally to this work. This work was supported by the National Key Research and Development Program of China (no.2022YFA1405000), the National Natural Science Foundation of China (no. RK106LH21001 and no. 22209214), the Natural Science Foundation of Jiangsu Province, Major Project (no. BK20212004), the Key Scientific Research Project in Colleges and Universities of Henan Province of China (no. 22A540001), and Incubation Program for Young Master Supervisor of Zhongyuan University of Technology (no. SD202218).

Conflict of Interest

The authors declare no conflict of interest.

Keywords

conductive hydrogels, construction strategies, flexible electronics, hydrogel fibers

Received: November 19, 2022
Revised: January 13, 2023
Published online:

[1] S. Choi, H. Lee, R. Ghaffari, T. Hyeon, D. H. Kim, *Adv. Mater.* **2016**, *28*, 4203.
[2] W. Gao, H. Ota, D. Kiriya, K. Takei, A. Javey, *Acc. Chem. Res.* **2019**, *52*, 523.
[3] W. Heng, S. Solomon, W. Gao, *Adv. Mater.* **2022**, *34*, 2107902.
[4] C. Hou, H. Wang, Q. Zhang, Y. Li, M. Zhu, *Adv. Mater.* **2014**, *26*, 5018.
[5] M. Magliulo, M. Mulla, M. Singh, E. Macchia, A. Tiwari, L. Torsi, K. Manoli, *J. Mater. Chem. C* **2015**, *3*, 12347.

[6] B. Nie, S. Liu, Q. Qu, Y. Zhang, M. Zhao, J. Liu, *Acta Biomater.* **2021**, *139*, 280.
[7] H. L. Park, Y. Lee, N. Kim, D. G. Seo, G. T. Go, T. W. Lee, *Adv. Mater.* **2020**, *32*, 1903558.
[8] P. Wang, M. Hu, H. Wang, Z. Chen, Y. Feng, J. Wang, W. Ling, Y. Huang, *Adv. Sci.* **2020**, *7*, 2001116.
[9] S. Huang, Y. Liu, Y. Zhao, Z. Ren, C. F. Guo, *Adv. Funct. Mater.* **2019**, *29*, 1805924.
[10] Y. Liu, K. He, G. Chen, W. R. Leow, X. Chen, *Chem. Rev.* **2017**, *117*, 12893.
[11] J. A. Rogers, T. Someya, Y. Huang, *Science* **2010**, *327*, 1603.
[12] X. Chen, J. A. Rogers, S. P. Lacour, W. Hu, D. H. Kim, *Chem. Soc. Rev.* **2019**, *48*, 1431.
[13] Y. Chen, Y. Zhang, Z. Liang, Y. Cao, Z. Han, X. Feng, *npj Flexible Electron.* **2020**, *4*, 1.
[14] H. Ling, S. Liu, Z. Zheng, F. Yan, *Small Methods* **2018**, *2*, 1800070.
[15] Z. Liu, J. Xu, D. Chen, G. Shen, *Chem. Soc. Rev.* **2015**, *44*, 161.
[16] Y. Sun, J. A. Rogers, *Adv. Mater.* **2007**, *19*, 1897.
[17] K. J. Yu, Z. Yan, M. Han, J. A. Rogers, *npj Flexible Electron.* **2017**, *1*, 4.
[18] E. M. Ahmed, *J. Adv. Res.* **2015**, *6*, 105.
[19] L. Ionov, *Mater. Today* **2014**, *17*, 494.
[20] J. Li, D. J. Mooney, *Nat. Rev. Mater.* **2016**, *1*, 1.
[21] X. Liu, J. Liu, S. Lin, X. Zhao, *Mater. Today* **2020**, *36*, 102.
[22] X. Yao, J. Liu, C. Yang, X. Yang, J. Wei, Y. Xia, X. Gong, Z. Suo, *Adv. Mater.* **2019**, *31*, 1903062.
[23] H. Yuk, B. Lu, X. Zhao, *Chem. Soc. Rev.* **2019**, *48*, 1642.
[24] A. Hirano, T. Tanaka, Y. Urabe, H. Kataura, *ACS Nano* **2013**, *7*, 10285.
[25] L. Y. Hsiao, L. Jing, K. Li, H. Yang, Y. Li, P. Y. Chen, *Carbon* **2020**, *161*, 784.
[26] J. H. Min, M. Patel, W. G. Koh, *Polymers* **2018**, *10*, 1078.
[27] P. Thoniyot, M. J. Tan, A. A. Karim, D. J. Young, X. J. Loh, *Adv. Sci.* **2015**, *2*, 1400010.
[28] L. Han, K. Liu, M. Wang, K. Wang, L. Fang, H. Chen, J. Zhou, X. Lu, *Adv. Funct. Mater.* **2018**, *28*, 1704195.
[29] S. J. Devaki, R. K. Narayanan, S. Sarojam, *Mater. Lett.* **2014**, *116*, 135.
[30] J. Duan, X. Liang, J. Guo, K. Zhu, L. Zhang, *Adv. Mater.* **2016**, *28*, 8037.
[31] K. Chen, Q. Ying, X. Hao, K. Sun, H. Wang, *Int. J. Bioprint.* **2021**, *7*, 377.
[32] T. Distler, A. R. Boccaccini, *Acta Biomater.* **2020**, *101*, 1.
[33] H. P. Lee, K. A. Deo, J. Jeong, M. Namkoong, K. Y. Kuan, L. Tian, A. K. Gaharwar, *Adv. Mater. Interfaces* **2022**, *9*, 2201186.
[34] S. Sayyar, E. Murray, B. Thompson, J. Chung, D. L. Officer, S. Gambhir, G. M. Spinks, G. G. Wallace, *J. Mater. Chem. B* **2015**, *3*, 481.
[35] M. Shin, K. H. Song, J. C. Burrell, D. K. Cullen, J. A. Burdick, *Adv. Sci.* **2019**, *6*, 1901229.
[36] F. Zhu, J. Lin, Z. L. Wu, S. Qu, J. Yin, J. Qian, Q. Zheng, *ACS Appl. Mater. Interfaces* **2018**, *10*, 13685.
[37] T. Cheng, Y. Z. Zhang, S. Wang, Y. L. Chen, S. Y. Gao, F. Wang, W. Y. Lai, W. Huang, *Adv. Funct. Mater.* **2021**, *31*, 2101303.
[38] S. Sardana, A. Gupta, K. Singh, A. Maan, A. Ohlan, *J. Energy Storage* **2021**, *45*, 103510.
[39] J. P. Xu, Y. L. Tsai, S. H. Hsu, *Molecules* **2020**, *25*, 5296.
[40] F. G. Torres, O. P. Troncoso, G. E. DelaTorre, *Int. J. Energy Res.* **2022**, *46*, 5603.
[41] H. Dechiraju, M. Jia, L. Luo, M. Rolandi, *Adv. Sustainable Syst.* **2022**, *6*, 2100173.
[42] X. Sun, F. Yao, J. Li, *J. Mater. Chem. A* **2020**, *8*, 18605.
[43] C. Li, *RSC Adv.* **2021**, *11*, 33835.
[44] B. Yao, H. Wang, Q. Zhou, M. Wu, M. Zhang, C. Li, G. Shi, *Adv. Mater.* **2017**, *29*, 1700974.
[45] C. Wang, S. Zhai, Z. Yuan, J. Chen, Z. Yu, Z. Pei, F. Liu, X. Li, L. Wei, Y. Chen, *Carbon* **2020**, *164*, 100.
[46] Q. Zhou, W. Teng, Y. Jin, L. Sun, P. Hu, H. Li, L. Wang, J. Wang, *Electrochim. Acta* **2020**, *334*, 135530.
[47] M. Li, X. Chen, X. Li, J. Dong, X. Zhao, Q. Zhang, *ACS Appl. Mater. Interfaces* **2021**, *13*, 43323.
[48] L. Fan, X. Ge, Y. Qian, M. Wei, Z. Zhang, W. E. Yuan, Y. Ouyang, *Front. Bioeng. Biotechnol.* **2020**, *8*, 654.
[49] X. Di, J. Li, M. Yang, Q. Zhao, G. Wu, P. Sun, *J. Mater. Chem. A* **2021**, *9*, 20703.
[50] G. Xiao, Y. Wang, H. Zhang, Z. Zhu, S. Fu, *Int. J. Biol. Macromol.* **2021**, *170*, 272.
[51] Y. Li, C. Hu, J. Lan, B. Yan, Y. Zhang, L. Shi, R. Ran, *Polymer* **2020**, *186*, 122027.
[52] Q. Zhou, J. Lyu, G. Wang, M. Robertson, Z. Qiang, B. Sun, C. Ye, M. Zhu, *Adv. Funct. Mater.* **2021**, *31*, 2104536.
[53] X. Zhang, J. Wei, S. Lu, H. Xiao, Q. Miao, M. Zhang, K. Liu, L. Chen, L. Huang, H. Wu, *ACS Appl. Polym. Mater.* **2021**, *3*, 5798.
[54] W. Wei, J. Liu, J. Huang, F. Cao, K. Qian, Y. Yao, W. Li, *Eur. Polym. J.* **2022**, *175*, 111385.
[55] L. Shuai, Z. H. Guo, P. Zhang, J. Wan, X. Pu, Z. L. Wang, *Nano Energy* **2020**, *78*, 105389.
[56] X. Zhang, J. Cai, W. Liu, W. Liu, X. Qiu, *Polymer* **2020**, *188*, 122147.
[57] X. Dai, Y. Long, B. Jiang, W. Guo, W. Sha, J. Wang, Z. Cong, J. Chen, B. Wang, W. Hu, *Nano Res.* **2022**, *15*, 5461.
[58] Q. Rong, W. Lei, M. Liu, *Chemistry* **2018**, *24*, 16930.
[59] C. Zhou, T. Wu, X. Xie, G. Song, X. Ma, Q. Mu, Z. Huang, X. Liu, C. Sun, W. Xu, *Eur. Polym. J.* **2022**, *177*, 111454.
[60] X. Guo, J. Li, F. Wang, J. H. Zhang, J. Zhang, Y. Shi, L. Pan, *J. Polym. Sci.* **2022**, *60*, 2635.
[61] Y. Shi, G. Yu, *Chem. Mater.* **2016**, *28*, 2466.
[62] W. Zhang, P. Feng, J. Chen, Z. Sun, B. Zhao, *Prog. Polym. Sci.* **2019**, *88*, 220.
[63] Z. Chen, Y. Chen, M. S. Hedenqvist, C. Chen, C. Cai, H. Li, H. Liu, J. Fu, *J. Mater. Chem. B* **2021**, *9*, 2561.
[64] Q. Peng, J. Chen, T. Wang, X. Peng, J. Liu, X. Wang, J. Wang, H. Zeng, *InfoMat* **2020**, *2*, 843.
[65] K. Liu, S. Wei, L. Song, H. Liu, T. Wang, *J. Agric. Food Chem.* **2020**, *68*, 7269.
[66] Y. Guo, J. Bae, F. Zhao, G. Yu, *Trends Chem.* **2019**, *1*, 335.
[67] Y. Li, J. Wang, Y. Wang, W. Cui, *Composites, Part B* **2021**, *223*, 109101.
[68] Y. Zhang, J. Ding, B. Qi, W. Tao, J. Wang, C. Zhao, H. Peng, J. Shi, *Adv. Funct. Mater.* **2019**, *29*, 1902834.
[69] R. Ansar, S. Saqib, A. Mukhtar, M. B. K. Niazi, M. Shahid, Z. Jahan, S. J. Kakar, B. Uzair, M. Mubashir, S. Ullah, K. S. Khoo, H. R. Lim, P. L. Show, *Chemosphere* **2022**, *287*, 131956.
[70] C. F. Guimarães, R. Ahmed, A. P. Marques, R. L. Reis, U. Demirci, *Adv. Mater.* **2021**, *33*, 2006582.
[71] M. Volpi, A. Paradiso, M. Costantini, W. Swieszkowski, *ACS Biomater. Sci. Eng.* **2022**, *8*, 379.
[72] S. Khorshidi, A. Karkhaneh, *J. Biomed. Mater. Res., Part A* **2018**, *106*, 718.
[73] B. W. Walker, R. P. Lara, E. Mogadam, C. H. Yu, W. Kimball, N. Annabi, *Prog. Polym. Sci.* **2019**, *92*, 135.
[74] R. Lv, Z. Bei, Y. Huang, Y. Chen, Z. Zheng, Q. You, C. Zhu, Y. Cao, *Macromol. Rapid Commun.* **2020**, *41*, 1900450.
[75] L. Zhang, J. Wang, S. Wang, L. Wang, M. Wu, *J. Mater. Chem. C* **2022**, *10*, 4327.
[76] W. Teng, Q. Zhou, X. Wang, H. Che, P. Hu, H. Li, J. Wang, *Chem. Eng. J.* **2020**, *390*, 124569.
[77] R. Ansar, S. Saqib, A. Mukhtar, M. B. K. Niazi, M. Shahid, Z. Jahan, S. J. Kakar, B. Uzair, M. Mubashir, S. Ullah, *Chemosphere* **2022**, *287*, 131956.
[78] M. Li, X. Chen, X. Li, J. Dong, X. Zhao, Q. Zhang, *ACS Appl. Mater. Interfaces* **2021**, *13*, 43323.

[79] E. Piantanida, G. Alonci, A. Bertucci, L. De Cola, *Acc. Chem. Res.* **2019**, *52*, 2101.
[80] Y. J. Heo, H. Shibata, T. Okitsu, T. Kawanishi, S. Takeuchi, *Proc. Natl. Acad. Sci.* **2011**, *108*, 13399.
[81] X. Han, G. Xiao, Y. Wang, X. Chen, G. Duan, Y. Wu, X. Gong, H. Wang, *J. Mater. Chem. A* **2020**, *8*, 23059.
[82] L. Li, J. Meng, M. Zhang, T. Liu, C. Zhang, *Chem. Commun.* **2022**, *58*, 185.
[83] B. Yao, H. Wang, Q. Zhou, M. Wu, M. Zhang, C. Li, G. Shi, *Adv. Mater.* **2017**, *29*, 1700974.
[84] L. Zhao, T. Xu, B. Wang, Z. Mao, X. Sui, X. Feng, *Chem. Eng. J.* **2022**, *455*, 140796.
[85] F. Wang, J. Chen, X. Cui, X. Liu, X. Chang, Y. Zhu, *ACS Appl. Mater. Interfaces* **2022**, *14*, 30268.
[86] L. Zhao, B. Wang, Z. Mao, X. Sui, X. Feng, *Chem. Eng. J.* **2022**, *433*, 133500.
[87] L. Sun, H. Huang, Q. Ding, Y. Guo, W. Sun, Z. Wu, M. Qin, Q. Guan, Z. You, *Adv. Fiber Mater.* **2022**, *4*, 98.
[88] L. Geng, S. Hu, M. Cui, J. Wu, A. Huang, S. Shi, X. Peng, *Carbohydr. Polym.* **2021**, *262*, 117936.
[89] P. Li, Z. Jin, L. Peng, F. Zhao, D. Xiao, Y. Jin, G. Yu, *Adv. Mater.* **2018**, *30*, 1800124.
[90] Q. Zhou, W. Teng, Y. Jin, L. Sun, P. Hu, H. Li, L. Wang, J. Wang, *Electrochim. Acta* **2020**, *334*, 135530.
[91] T. Xu, D. Yang, S. Zhang, T. Zhao, M. Zhang, Z. Yu, *Carbon* **2021**, *171*, 201.
[92] Y. Li, X. Zhang, *Adv. Funct. Mater.* **2022**, *32*, 2107767.
[93] W. Shi, Z. Wang, H. Song, Y. Chang, W. Hou, Y. Li, G. Han, *ACS Appl. Mater. Interfaces* **2022**, *14*, 35114.
[94] X. Zhao, F. Chen, Y. Li, H. Lu, N. Zhang, M. Ma, *Nat. Commun.* **2018**, *9*, 3579.
[95] X. Duan, J. Yu, Y. Zhu, Z. Zheng, Q. Liao, Y. Xiao, Y. Li, Z. He, Y. Zhao, H. Wang, *ACS Nano* **2020**, *14*, 14929.
[96] M. Ju, B. Wu, S. Sun, P. Wu, *Adv. Funct. Mater.* **2020**, *30*, 1910387.
[97] Z. Deng, R. Yu, B. Guo, *Mater. Chem. Front.* **2021**, *5*, 2092.
[98] J. Shang, P. Theato, *Soft Matter* **2018**, *14*, 8401.
[99] A. Roy, K. Manna, S. Pal, *Mater. Chem. Front.* **2022**, *6*, 2338.
[100] D. Zhang, B. Ren, Y. Zhang, L. Xu, Q. Huang, Y. He, X. Li, J. Wu, J. Yang, Q. Chen, *J. Mater. Chem. B* **2020**, *8*, 3171.
[101] Z. Deng, H. Wang, P. X. Ma, B. Guo, *Nanoscale* **2020**, *12*, 1224.
[102] X. Ren, M. Yang, T. Yang, C. Xu, Y. Ye, X. Wu, X. Zheng, B. Wang, Y. Wan, Z. Luo, *ACS Appl. Mater. Interfaces* **2021**, *13*, 25374.
[103] X. Sui, H. Guo, C. Cai, Q. Li, C. Wen, X. Zhang, X. Wang, J. Yang, L. Zhang, *Chem. Eng. J.* **2021**, *419*, 129478.
[104] S. Li, Y. Cong, J. Fu, *J. Mater. Chem. B* **2021**, *9*, 4423.
[105] D. L. Taylor, M. in het Panhuis, *Adv. Mater.* **2016**, *28*, 9060.
[106] P. He, J. Wu, X. Pan, L. Chen, K. Liu, H. Gao, H. Wu, S. Cao, L. Huang, Y. Ni, *J. Mater. Chem. A* **2020**, *8*, 3109.
[107] Y. Jian, S. Handschuh-Wang, J. Zhang, W. Lu, X. Zhou, T. Chen, *Mater. Horiz.* **2021**, *8*, 351.
[108] Y. Guo, J. Bae, Z. Fang, P. Li, F. Zhao, G. Yu, *Chem. Rev.* **2020**, *120*, 7642.
[109] Q. Guan, Z. Han, Y. Zhu, W. Xu, H. Yang, Z. Ling, B. Yan, K. Yang, C. Yin, H. Wu, *Nano Lett.* **2021**, *21*, 952.
[110] X. Zhao, X. Sun, L. Yildirimer, Q. Lang, Z. Y. W. Lin, R. Zheng, Y. Zhang, W. Cui, N. Annabi, A. Khademhosseini, *Acta Biomater.* **2017**, *49*, 66.
[111] M. Akbari, A. Tamayol, V. Laforte, N. Annabi, A. H. Najafabadi, A. Khademhosseini, D. Juncker, *Adv. Funct. Mater.* **2014**, *24*, 4060.
[112] A. K. Yetisen, N. Jiang, A. Fallahi, Y. Montelongo, G. U. Ruiz Esparza, A. Tamayol, Y. S. Zhang, I. Mahmood, S. A. Yang, K. S. Kim, *Adv. Mater.* **2017**, *29*, 1606380.
[113] J. Guo, X. Liu, N. Jiang, A. K. Yetisen, H. Yuk, C. Yang, A. Khademhosseini, X. Zhao, S. H. Yun, *Adv. Mater.* **2016**, *28*, 10244.
[114] M. Elsherif, M. U. Hassan, A. K. Yetisen, H. Butt, *Biosens. Bioelectron.* **2019**, *137*, 25.
[115] G. Chen, G. Wang, X. Tan, K. Hou, Q. Meng, P. Zhao, S. Wang, J. Zhang, Z. Zhou, T. Chen, *Natl. Sci. Rev.* **2021**, *8*, 209.
[116] T. Chen, X. Qiao, P. Wei, G. Chen, I. T. Mugaanire, K. Hou, M. Zhu, *Chem. Mater.* **2020**, *32*, 9675.
[117] S. Xu, Y. Yan, Y. Zhao, X. Qiu, D. Zhuang, H. Liu, X. Cui, J. Huang, X. Wu, C. Huang, *J. Mater. Chem. C* **2021**, *9*, 5554.
[118] L. Wu, L. Li, M. Fan, P. Tang, S. Yang, L. Pan, H. Wang, Y. Bin, *Composites, Part A* **2020**, *138*, 106050.
[119] C. You, W. Qin, Z. Yan, Z. Ren, J. Huang, J. Ii, W. Chang, W. He, K. Wen, S. Yin, *J. Mater. Chem. A* **2021**, *9*, 10240.
[120] T. Chen, P. Wei, G. Chen, H. Liu, I. T. Mugaanire, K. Hou, M. Zhu, *J. Mater. Chem. A* **2021**, *9*, 12265.
[121] A. Leber, C. Dong, R. Chandran, T. Das Gupta, N. Bartolomei, F. Sorin, *Nat. Electron.* **2020**, *3*, 316.
[122] G. Loke, W. Yan, T. Khudiyev, G. Noel, Y. Fink, *Adv. Mater.* **2020**, *32*, 1904911.
[123] Y. Qu, T. N. Dang, A. G. Page, W. Yan, T. D. Gupta, G. M. Rotaru, R. M. Rossi, V. D. Favrod, N. Bartolomei, F. Sorin, *Adv. Mater.* **2018**, *30*, 1707251.
[124] P. Wei, K. Hou, T. Chen, G. Chen, I. T. Mugaanire, M. Zhu, *Mater. Horiz.* **2020**, *7*, 811.
[125] X. Hu, K. Vasanthavada, K. Kohler, S. McNary, A. Moore, C. Vierra, *Cell. Mol. Life Sci.* **2006**, *63*, 1986.
[126] M. Andersson, J. Johansson, A. Rising, *Int. J. Mol. Sci.* **2016**, *17*, 1290.
[127] J. Song, S. Chen, L. Sun, Y. Guo, L. Zhang, S. Wang, H. Xuan, Q. Guan, Z. You, *Adv. Mater.* **2020**, *32*, 1906994.
[128] J. Chen, H. Wen, G. Zhang, F. Lei, Q. Feng, Y. Liu, X. Cao, H. Dong, *ACS Appl. Mater. Interfaces* **2020**, *12*, 7565.
[129] Y. He, N. Zhang, Q. Gong, H. Qiu, W. Wang, Y. Liu, J. Gao, *Carbohydr. Polym.* **2012**, *88*, 1100.
[130] Y. An, L. Gao, T. Wang, *ACS Appl. Nano Mater.* **2020**, *3*, 5079.
[131] J. Fei, Z. Zhang, L. Zhong, L. Gu, *J. Appl. Polym. Sci.* **2002**, *85*, 2423.
[132] Y. Cheng, Y. Yu, F. Fu, J. Wang, L. Shang, Z. Gu, Y. Zhao, *ACS Appl. Mater. Interfaces* **2016**, *8*, 1080.
[133] T. Y. Lee, M. Ku, B. Kim, S. Lee, J. Yang, S. H. Kim, *Small* **2017**, *13*, 1700646.
[134] Y. Jun, E. Kang, S. Chae, S. H. Lee, *Lab Chip* **2014**, *14*, 2145.
[135] J. Guo, Y. Yu, L. Cai, Y. Wang, K. Shi, L. Shang, J. Pan, Y. Zhao, *Mater. Today* **2021**, *44*, 105.
[136] X. Y. Du, Q. Li, G. Wu, S. Chen, *Adv. Mater.* **2019**, *31*, 1903733.
[137] L. Shang, Y. Yu, Y. Liu, Z. Chen, T. Kong, Y. Zhao, *ACS Nano* **2019**, *13*, 2749.
[138] P. Xu, R. Xie, Y. Liu, G. Luo, M. Ding, Q. Liang, *Adv. Mater.* **2017**, *29*, 1701664.
[139] L. Peng, Y. Liu, J. Gong, K. Zhang, J. Ma, *RSC Adv.* **2017**, *7*, 19243.
[140] M. Zhou, J. Gong, J. Ma, *e-Polym.* **2019**, *19*, 215.
[141] J. Cai, D. Ye, Y. Wu, L. Fan, H. Yu, *Compos. Commun.* **2019**, *15*, 1.
[142] Y. Wu, L. Wang, B. Guo, P. X. Ma, *ACS Nano* **2017**, *11*, 5646.
[143] C. M. Hwang, A. Khademhosseini, Y. Park, K. Sun, S. H. Lee, *Langmuir* **2008**, *24*, 6845.
[144] B. G. Chung, K. H. Lee, A. Khademhosseini, S. H. Lee, *Lab Chip* **2012**, *12*, 45.
[145] L. Peng, Y. Liu, J. Huang, J. Li, J. Gong, J. Ma, *Eur. Polym. J.* **2018**, *103*, 335.
[146] X. Duan, J. Yu, Y. Zhu, Z. Zheng, Q. Liao, Y. Xiao, Y. Li, Z. He, Y. Zhao, H. Wang, L. Qu, *ACS Nano* **2020**, *14*, 14929.
[147] S. Wei, G. Qu, G. Luo, Y. Huang, H. Zhang, X. Zhou, L. Wang, Z. Liu, T. Kong, *ACS Appl. Mater. Interfaces* **2018**, *10*, 11204.
[148] Z. Al Dulimi, M. Wallis, D. K. Tan, M. Maniruzzaman, A. Nokhodchi, *Drug Discovery Today* **2020**, *26*, 360.
[149] D. Fan, Y. Li, X. Wang, T. Zhu, Q. Wang, H. Cai, W. Li, Y. Tian, Z. Liu, *Front. Pharmacol.* **2020**, *11*, 122.

[150] N. Shahrubudin, T. C. Lee, R. Ramlan, *Procedia Manuf.* **2019**, *35*, 1286.
[151] A. De Mori, M. Peña Fernández, G. Blunn, G. Tozzi, M. Roldo, *Polymers* **2018**, *10*, 285.
[152] T. S. Jang, H. D. Jung, H. M. Pan, W. T. Han, S. Chen, J. Song, *Int. J. Bioprint.* **2018**, *4*, 126.
[153] H. Li, C. Tan, L. Li, *Mater. Des.* **2018**, *159*, 20.
[154] D. Wu, N. H. Vonk, B. A. Lamers, M. Castilho, J. Malda, J. P. Hoefnagels, P. Y. Dankers, *Eur. Polym. J.* **2020**, *141*, 110099.
[155] Y. Wu, Y. Zeng, Y. Chen, C. Li, R. Qiu, W. Liu, *Adv. Funct. Mater.* **2021**, *31*, 2107202.
[156] X. Zhang, Q. Zheng, Z. L. Wu, *Composites, Part B* **2022**, *238*, 109895.
[157] Z. Lei, Q. Wang, P. Wu, *Mater. Horiz.* **2017**, *4*, 694.
[158] D. N. Heo, S. J. Lee, R. Timsina, X. Qiu, N. J. Castro, L. G. Zhang, *Mater. Sci. Eng., C* **2019**, *99*, 582.
[159] F. Zhu, L. Cheng, J. Yin, Z. Wu, J. Qian, J. Fu, Q. Zheng, *ACS Appl. Mater. Interfaces* **2016**, *8*, 31304.
[160] Y. Chen, M. Shafiq, M. Liu, Y. Morsi, X. Mo, *Bioact. Mater.* **2020**, *5*, 963.
[161] T. Subbiah, G. S. Bhat, R. W. Tock, S. Parameswaran, S. S. Ramkumar, *J. Appl. Polym. Sci.* **2005**, *96*, 557.
[162] W. E. Teo, R. Inai, S. Ramakrishna, *Sci. Technol. Adv. Mater.* **2011**, *12*, 013002.
[163] C. Chen, J. Tang, Y. Gu, L. Liu, X. Liu, L. Deng, C. Martins, B. Sarmento, W. Cui, L. Chen, *Adv. Funct. Mater.* **2019**, *29*, 1806899.
[164] M. G. Grewal, C. B. Highley, *Biomater. Sci.* **2021**, *9*, 4228.
[165] K. Molnar, A. Jedlovszky Hajdu, M. Zrinyi, S. Jiang, S. Agarwal, *Macromol. Rapid Commun.* **2017**, *38*, 1700147.
[166] Y. Yang, C. Wang, C. G. Wiener, J. Hao, S. Shatas, R. Weiss, B. D. Vogt, *ACS Appl. Mater. Interfaces* **2016**, *8*, 22774.
[167] L. Wang, Y. Wu, T. Hu, P. X. Ma, B. Guo, *Acta Biomater.* **2019**, *96*, 175.
[168] D. O. Miranda, M. F. Dorneles, R. L. Orefice, *Polymer* **2020**, *200*, 122590.
[169] F. M. Al Oqla, S. Sapuan, T. Anwer, M. Jawaid, M. Hoque, *Synth. Met.* **2015**, *206*, 42.
[170] W. Zeng, L. Shu, Q. Li, S. Chen, F. Wang, X. M. Tao, *Adv. Mater.* **2014**, *26*, 5310.
[171] X. Zhang, H. Lin, H. Shang, J. Xu, J. Zhu, W. Huang, *SusMat* **2021**, *1*, 105.
[172] J. Liu, Y. Jia, Q. Jiang, F. Jiang, C. Li, X. Wang, P. Liu, P. Liu, F. Hu, Y. Du, *ACS Appl. Mater. Interfaces* **2018**, *10*, 44033.
[173] Y. W. Chong, W. Ismail, K. Ko, C. Y. Lee, *IEEE Sens. J.* **2019**, *19*, 9047.
[174] A. Nechibvute, A. Chawanda, P. Luhanga, *Smart Mater. Res.* **2012**, *2012*, 853481.
[175] A. Nozariasbmarz, H. Collins, K. Dsouza, M. H. Polash, M. Hosseini, M. Hyland, J. Liu, A. Malhotra, F. M. Ortiz, F. Mohaddes, *Appl. Energy* **2020**, *258*, 114069.
[176] K. V. Selvan, M. S. M. Ali, *Renewable Sustainable Energy Rev.* **2016**, *54*, 1035.
[177] J. Tian, X. Chen, Z. Wang, *Nanotechnology* **2020**, *31*, 242001.
[178] B. Chen, W. Tang, T. Jiang, L. Zhu, X. Chen, C. He, L. Xu, H. Guo, P. Lin, D. Li, *Nano Energy* **2018**, *45*, 380.
[179] T. Ding, Y. Zhou, X. Wang, C. Zhang, T. Li, Y. Cheng, W. Lu, J. He, G. W. Ho, *Adv. Energy Mater.* **2021**, *11*, 2102219.
[180] L. Dong, M. Wang, J. Wu, C. Zhu, J. Shi, H. Morikawa, *Adv. Fiber Mater.* **2022**, *4*, 1486.
[181] Y. Lin, J. Liu, X. Wang, J. Xu, P. Liu, G. Nie, C. Liu, F. Jiang, *Compos. Commun.* **2019**, *16*, 79.
[182] X. Wang, K. H. Chan, W. Lu, T. Ding, S. W. L. Ng, Y. Cheng, T. Li, M. Hong, B. C. Tee, G. W. Ho, *Nat. Commun.* **2022**, *13*, 1.
[183] Q. Huang, D. Wang, Z. Zheng, *Adv. Energy Mater.* **2016**, *6*, 1600783.
[184] A. Sumboja, J. Liu, W. G. Zheng, Y. Zong, H. Zhang, Z. Liu, *Chem. Soc. Rev.* **2018**, *47*, 5919.
[185] D. Chen, K. Jiang, T. Huang, G. Shen, *Adv. Mater.* **2020**, *32*, 1901806.
[186] M. Liao, L. Ye, Y. Zhang, T. Chen, H. Peng, *Adv. Electron. Mater.* **2019**, *5*, 1800456.
[187] S. Senthilkumar, Y. Wang, H. Huang, *J. Mater. Chem. A* **2015**, *3*, 20863.
[188] D. Yu, Q. Qian, L. Wei, W. Jiang, K. Goh, J. Wei, J. Zhang, Y. Chen, *Chem. Soc. Rev.* **2015**, *44*, 647.
[189] Z. Zhang, F. Xiao, S. Wang, *J. Mater. Chem. A* **2015**, *3*, 11215.
[190] R. Jia, L. Li, Y. Ai, H. Du, X. Zhang, Z. Chen, G. Shen, *Sci. China Mater.* **2018**, *61*, 254.
[191] S. Han, H. Peng, Q. Sun, S. Venkatesh, K. S. Chung, S. C. Lau, Y. Zhou, V. Roy, *Adv. Mater.* **2017**, *29*, 1700375.
[192] N. Wen, L. Zhang, D. Jiang, Z. Wu, B. Li, C. Sun, Z. Guo, *J. Mater. Chem. A* **2020**, *8*, 25499.
[193] X. Wang, X. Wang, M. Pi, R. Ran, *Chem. Eng. J.* **2022**, *428*, 131172.
[194] Y. Y. Lee, H. Y. Kang, S. H. Gwon, G. M. Choi, S. M. Lim, J. Y. Sun, Y. C. Joo, *Adv. Mater.* **2016**, *28*, 1636.
[195] T. Yin, L. Wu, T. Wu, G. Mao, G. Nian, Z. Chen, X. Hu, P. Wang, Y. Xiang, H. Yu, *J. Polym. Sci., Part B: Polym. Phys.* **2019**, *57*, 272.
[196] Y. J. Jo, S. Y. Kim, J. H. Hyun, B. Park, S. Choy, G. R. Koirala, T. i. Kim, *npj Flexible Electron.* **2022**, *6*, 31.
[197] S. Zhang, Y. Chen, H. Liu, Z. Wang, H. Ling, C. Wang, J. Ni, B. Çelebi Saltik, X. Wang, X. Meng, *Adv. Mater.* **2020**, *32*, 1904752.
[198] M. Zhang, S. Chen, N. Sheng, B. Wang, Z. Wu, Q. Liang, Z. Han, H. Wang, *J. Mater. Chem. A* **2021**, *9*, 12574.
[199] B. Mirani, E. Pagan, S. Shojaei, S. M. H. Dabiri, H. Savoji, M. Mehrali, M. Sam, J. Alsaif, R. B. Bhiladvala, A. Dolatshahi Pirouz, *ACS Appl. Mater. Interfaces* **2020**, *12*, 9080.

Wanwan Li received her Ph.D. degree at School of Chemistry and Materials Science, University of Science and Technology of China in 2018. She is currently a lecturer at Zhongyuan University of Technology. Her current scientific interests mainly focus on the design, construction, and applications of conductive hydrogel materials for flexible/wearable multifunctional electronics.

Jiao Liu received her Ph.D. degree in Advanced Material and Liquid Crystal Institute (AMLCI) at Kent State University in 2022. She is currently a lecturer at Nanjing University of Posts and Telecommunications. Her research is mainly focused on the stimuli-responsive soft matter of soft material, liquid crystal elastomer/polymer, and ferroelectric nematic liquid crystals.

Bingxiang Li received his Ph.D. degree in Advanced Material and Liquid Crystal Institute (AMLCI) at Kent State University in 2019. He is currently a professor at Nanjing University of Posts and Telecommunications. His research is mainly focused on the liquid crystal, the stimuli-responsive soft matter, active matter, biological physics.